Expression, purification and characterization of recombinant RNA-dependent RNA polymerase from Heterobasidion RNA virus 6

Alesia Levanova
Master's thesis
Department of Chemistry
Faculty of Science
University of Turku
April 2022

The originality of this thesis has been checked in accordance with the University of Turku quality assurance system using the Turnitin OriginalityCheck service

UNIVERSITY of TURKU
Faculty of Science
LEVANOVA ALESIA: Expression, purification and characterization of recombinant RNA-dependent RNA polymerase from Heterobasidion RNA virus 6
Master's thesis 37 pages
Department of Chemistry
April 2022

RNA-dependent RNA polymerases (RdRps) are enzymes that catalyze nucleotide polymerization on RNA template in the presence of divalent metal ions. These enzymes are central for the life cycle of viruses with RNA genomes. A double-stranded RNA (dsRNA) mycovirus Heterobasidion RNA virus 6 (HetRV6) commonly infect forest pathogenic fungi from the species complex *Heterobasidion annosum* sensu lato. In general, the infection caused by HetRV6 is cryptic, but sometimes have negative or mutualistic impact on its host. The understanding of the HetRV6 life cycle, including RNA synthesis, can shed light on the biology of HetRV6 virus and explain its divergent impacts on the host. Furthermore, a recombinant HetRV6 RdRp can potentially be harnessed to produce dsRNA molecules applicable for silencing of the target genes in plants, fungi, insects and mammals via RNA interference (RNAi).

The aim of the current study was to express, purify and characterize the *in vitro* enzymatic activities of RdRp from the HetRV6 virus. To this end, a complementary DNA sequence of the RdRp gene was cloned into *Escherichia coli* expression vector, from which the recombinant polymerase was expressed and purified using affinity, ion-exchange and size-exclusion chromatography. The purified HetRV6 RdRp was a soluble and active *in vitro* enzyme, which possesses polymerase and terminal nucleotidyl transferase (TNTase) activities in the absence of any primers or accessory viral or host proteins. The impact of the buffer composition, pH, temperature, divalent cations and nucleoside triphosphate concentrations was studied and the optimal reaction conditions were identified. The polymerase is fully dependent on Mn^{2+} ions and does not produce dsRNA in its absence, while Mg^{2+} ions at concentration 1–5 mM enhance the polymerization activity. HetRV6 polymerase is active on heterologous templates. However, the requirements for successful initiation and elongation should be still studied in more detail to fully understand how the enzyme can be used for efficient dsRNA synthesis for biotechnological applications. The discovered TNTase activity can potentially be used for *in vitro* RNA labeling.

The completed work is a useful starting point to further explore the properties of the HetRV6 RdRp in terms of possible RNA modifying tools, its structural organization and role in infection and host-microbe interactions.

Keywords: viral RNA-dependent RNA polymerase, protein purification, TNTase activity

Table of Contents

ABBREVIATIONS

ATP	adenosine triphosphate
bp	base pair
cDNA	complementary DNA
CTP	cytidine triphosphate
CV	column volume
DdRp	DNA-dependent RNA polymerase
DNase	deoxyribonuclease
DTT	dithiothreitol
dsRNA	double-stranded RNA
E. coli	*Escherichia coli*
EDTA	ethylenediaminetetraacetic acid
GTP	guanosine triphosphate
HetRV6	Heterobasidion RNA virus 6
IMAC	immobilized metal affinity chromatography
IPTG	isopropyl β-D-1-thiogalactopyranoside
luc	luciferase
Me	metal ion
mRNA	messenger RNA
MWCO	molecular weight cut-off
nt	nucleotide
NTP	nucleoside triphosphate
OD_{600}	optical density measured at λ=600 nm
PBV	picobirnavirus
PCR	polymerase chain reaction
PVDF	polyvinylidene fluoride
RdRp	RNA-dependent RNA polymerase
RNAi	RNA interference
RNase	ribonuclease
SDS-PAGE	sodium dodecyl sulphate polyacrylamide gel electrophoresis
SEC	size-exclusion chromatography
siRNA	small interfering RNA
ssRNA	single-stranded RNA
(-)ssRNA	negative-sense single-stranded RNA
(+)ssRNA	positive-sense single-stranded RNA
TBE	tris/borate/EDTA
TNTase activity	terminal nucleotidyl transferase activity
UTP	uridine triphosphate

1. INTRODUCTION

Viruses are obligate intracellular parasites, which infect organisms from all domains of life and are generally associated with severe diseases of humans and animals. However, most viruses do not cause any signs of illness and some of them even may establish symbiotic relationships with their hosts (Marquez et al., 2007). Some viruses have oncolytic properties; others can be used as vectors in gene therapy or serve as efficient vaccines (Mietzsch et al., 2017). Viruses are biochemically much more simpler than any cell and their studies have contributed a lot to the current understanding of cellular functions and disease mechanisms (Enquist, 2009).

Most viruses keep their genetic information in the form of RNA molecules. The genome of RNA viruses can consist of double-stranded RNA (dsRNA) or single-stranded RNA (ssRNA). The genome of ssRNA viruses can be further divided into positive sense RNA [(+)ssRNA], which is directly translated into viral proteins, and negative sense RNA [(-)ssRNA], which needs to be converted into (+)ssRNA for translation. RNA viruses use different strategies for genome replication (Voyles, 2002). However, all of them carry metal-activated template-dependent RNA-dependent RNA polymerases (RdRp).

The majority of RdRps contain a signature motif for RNA polymerases, glycine-aspartate-aspartate (GDD) amino acid sequence (Choi, 2012). However, variabilities in this conserved motif are possible. Thus, RdRps from cystoviruses contain SDD sequence instead of GDD (Alphonse and Ghose, 2017), while birnaviruses keep only part of the catalytic triad, DD amino acids (Shwed et al., 2002). Structurally all RdRps are similar to each other as well as to DNA-dependent RNA polymerases (DdRp), reverse transcriptases and DNA-dependent DNA polymerases (Ahlquist, 2002). They all look like a right hand with distinguishable fingers, palm and thumb subdomains and share a conserved catalytic core of 231 amino acids (Mönttinen et al., 2021), which provides correct positioning of the template, metal ions and incoming NTPs required for RNA synthesis. In contrast to “open hand” shape of other polymerases, most viral RdRp have a “closed hand” conformation, which is achieved by interconnections between the fingers and thumb domains with several loops creating two positively charged channels for the template and for the NTPs (Venkataraman et al., 2018). Seven conserved structural motifs (A–G) have been identified in all viral RdRps studied to date (Jácome et al., 2015). Motifs A to E can be found in the palm subdomain consisting of four antiparallel ß-strands and two α-helices, while motifs F and G are located in the fingers subdomain (Jácome et al., 2015; Venkataraman et al., 2018). The motifs A and C contain catalytic aspartates required for coordination of the catalytic ions, typically Mn^{2+} or Mg^{2+} (Genna et al., 2018; Steitz, 1998). Additionally a motif H has been discovered in the thumb subdomain of (+)ssRNA and dsRNA viruses (Černý et al., 2014).

During viral infection, RdRps are involved in a number of functions, such as; (1) recognition of the template RNAs, (2) genomic RNA replication and mRNA transcription, (3) possible modifications of the newly synthesized RNAs. Viral RdRps operate in specific environments that make possible different steps of RNA synthesis. Thus, in case of (-)ssRNA viruses, only viral RNAs coated with nucleocapsid protein can be efficiently used as a template for RdRp (Morin et al., 2013). In dsRNA viruses, RNA synthesis occurs inside a nucleocapsid (Poranen et al., 2001). RdRp of (+)ssRNA viruses operate in specific cytoplasmic compartments, where viral components efficiently concentrate (Novoa et al., 2005).

The RNA synthesis can be initiated either *de novo* or via a primer extension. In both cases, the formation of initiation complex requires RdRp, suitable RNA template, the first initiating nucleoside triphosphate (NTP_i) and the second NTP (NTP_{i+1}). In *de novo* initiation, an NTP_i serves similar to a primer providing its 3'-hydroxyl for the reaction with the incoming NTP. In most cases, *de novo* initiation is followed by elongation. However, sometimes it might result in the synthesis of short abortive RNA products that subsequently serve as primers (Kao et al., 2001; van Dijk et al., 2004). Furthermore, oligonucleotide primers can originate from a cleavage of a 5' capped cellular mRNA, so called "cap-snatching", actively used by (-)ssRNA viruses with segmented genome (Kao et al., 2001). When the 3'terminus of the template RNA folds back on itself, the 3' hydroxyl group of the template can be used as a primer, so called back-priming (Laurila et al., 2002). Picornaviruses use a protein primer, where an amino acid, such as tyrosine, provides a hydroxyl group for the reaction with the first NTP (Paul and Wimmer, 2015).

In addition to its functions related to RNA synthesis, viral RdRps promote genetic variability via the high rates of mutations during replication and, thus, drive viral evolution. RNA polymerase incorporates one wrong nucleotide per 10^3–10^7 nucleotides or one error occurs in each replicated genome (Choi, 2012). This high mutation rates allow rapid evolution under selective pressure caused by immune response of host organisms or drug treatments. Furthermore, RdRp is capable of RNA recombination by occasional template switching, which allow RNA viruses to rearrange their genomes, obtain new genes and repair deleterious mutations (Ahlquist, 2002).

Viral RdRps capable of *de novo* initiation of RNA synthesis and having high processivity, such as bacteriophage phi6 RdRp (van Dijk et al., 2004), have significant biotechnological potential since such RdRps alongside DdRps from bacteriophages T3, T7 or SP6 can be applied to synthesize large amounts of dsRNA for RNA interference (RNAi, Aalto et al., 2007). RNAi is a conserved mechanism of gene silencing in virtually all eukaryotes, which is accomplished by a sequence-specific binding of short dsRNAs in complex with Argonaute protein to a target mRNA resulting in mRNA degradation or translational repression. The enzymatically produced dsRNAs are currently

perceived as a valuable alternative to chemical pesticides, fungicides and antiviral agents for RNAi-based crop protection (Christiaens et al., 2020; Fletcher et al., 2020; Hernández-Soto and Chacón-Cerdas, 2021). Furthermore, the exogenous long dsRNA molecules can be cleaved *in vitro* by RNaseIII family enzyme Dicer into small interfering RNAs (siRNA), mediators of RNA interference (RNAi) in mammals. To prevent mammalian cell death, enzymatically generated siRNAs should be purified using anion-exchange chromatography (Romanovskaya et al., 2013), ion pair reverse-phase chromatography (Nwokeoji et al., 2017) or asymmetrical flow-field flow fractionation (Levanova et al., 2022) to a high level of purity. The exogenously prepared siRNAs can be delivered to mammalian cells, where they switch off the target gene activity (Elbashir et al., 2001). Three siRNA drugs against rare hereditary diseases have been recently approved, and many siRNA-based therapies aiming to treat severe incurable diseases are being developed (Saw and Song, 2020).

Newly discovered RdRps may be used as RNA processing and modification tools providing they possess corresponding enzymatic activities. Among such activities of RdRp is, for instance, terminal nucleotidyl transferase (TNTase) activity, which can be applied for 3' end labeling of RNA molecules. This activity has been reported for hepatitis C virus RdRp (Hong et al., 2001), phi6 RdRp (Poranen et al., 2008a), RdRp from human picobirnabirus (Collier et al., 2016). The biochemical properties of new viral RdRps can highlight future possible biotechnological applications. Furthermore, the RdRps from medically important viruses are potential pharmacological targets, while structural information obtained from various viral RdRps can help to solve basic biological questions and deduce evolutionary history of RNA viruses (Mönttinen et al., 2021).

In the current work, I will focus on the RdRp from a mycovirus infecting fungi belonging to basidiomycetous *Heterobasidion annosum* sensu lato species complex, which includes notorious parasites of boreal forests causing white rot diseases of spruces and pines (Garbelotto and Gonthier, 2013). About 15% of *Heterobasidion* isolates in Europe, Asia and North America carry one or more dsRNA viruses (Vainio et al., 2011). Heterobasidion RNA virus 6 (HetRV6) discovered in 2012 presents in 70% of all infected European isolates of *Heterobasidion* (Vainio et al., 2012). The HetRV6 effects on the fungus host growth are host- and temperature-dependent and can be beneficial, neutral or detrimental (Hyder, 2013). The amino acid sequence of HetRV6 is very different from the other viruses isolated from *Heterobasidion* fungi and it has been only recently taxonomically assigned to a newly created family *Orthocurvulaviridae*, genus *Orthocurvulavirus.* The genome of the HetRV6 comprises two dsRNA segments: 2050 base pairs (bp) long dsRNA1 encoding RdRp and 1859 bp long dsRNA2 coding for a putative capsid protein (Vainio et al., 2020). When I started my work, the HetRV6 RdRp was only identified as a putative polymerase based on the bioinformatics discovery of

conserved amino acid sequence motifs associated with viral RdRps (Vainio et al., 2012), and experimental data confirming the nature of this putative protein did not exist.

I expressed and purified a recombinant HetRV6 RdRp to show that the enzyme indeed possesses activities relevant to viral RdRps. HetRV6 RdRp is an active replicase *in vitro* capable of templated (replicase activity) and non-templated (TNTase activity) nucleotide addition. The enzyme does not require a primer or any additional viral or host proteins to synthesize a complementary strand on a (+)ssRNA template. HetRV6 RdRp is capable of *de novo* initiation on both native and heterologous templates. Its enzymatic activity is more dependent on Mn^{2+} rather than on Mg^{2+} ions *in vitro*. The polymerization is more efficient when concentration of adenine, the second nucleotide to be incorporated into the nascent RNA chain is increased, which poses the question about role of adenine in the initiation mechanism.

2. MATERIALS AND METHODS

2.1. Cloning, expression and purification of full-length RdRp from HetRV6 mycovirus

2.1.1. Preparation of the expression bacterial strains and bacterial lysate

To construct an expression plasmid, the HetRV6 RdRp gene (GenBank accession number HQ189459) was PCR-amplified from pCR2.1-TOPO_HetRV6_dsRNA1 cloning vector (Vainio et al., 2012) with high-fidelity Phusion DNA polymerase (ThermoFischer Scientific) using oligonucleotides presented in the appendix 1. The PCR product was treated with the restriction enzymes *NcoI* and *HindIII* (FastDigest, ThermoFisher Scientific), purified with NucleoSpin Gel and PCR Clean-up kit (Macherey Nagel), and ligated with the *NcoI-HindIII* and gel-purified Novogen expression vectors pET-32b(+) or pET-28a(+), to express the target protein with or without the N-terminal His-tag, respectively. After cloning, the sequence of the entire HetRV6 RdRp was confirmed in both constructs by Sanger sequencing (DNA sequencing service, University of Helsinki). Chemically competent *Escherichia coli* BL21(DE3)pLysS cells (Novagen) were transformed with the expression plasmids to give recombinant HetRV6 RdRp producing strains, designated as BL21(DE3)pLysS/His-HetRV6pol and BL21(DE3)pLysS/HetRV6pol.

To get expression of the recombinant polymerase, a starter culture of BL21(DE3)pLysS/His-HetRV6pol or BL21(DE3)pLysS/HetRV6pol in Luria-Bertani (LB) medium containing 25 µg/ml kanamycin was grown at 37°C with shaking until OD_{600} was ~0.5 followed by 50-fold dilution with the LB medium containing 40 µg/ml kanamycin to a final volume of 3 L. The diluted culture was further grown at 37°C with shaking to an $OD_{600}\approx0.9$. The culture was cooled on ice at 4°C before the induction with 0.5 mM isopropyl-β-D-thiogalactopyranoside (IPTG, Sigma-Aldrich). After that, the cells were incubated at 17°C for 18 h with shaking. Bacteria were pelleted and resuspended in 30 ml

lysis buffer [50 mM sodium phosphate pH 8.0, 100 mM NaCl (Sigma-Aldrich), 1 mM irreversible serine protease inhibitor Pefablock (Sigma-Aldrich)]. The suspension was sonicated on ice using the ultrasonic processor UP400S (Dr. Hielscher GmbH) three times 20 s×70% amplitude/0.5 cycle with 15 s breaks to cool the samples between cycles. The lysate was clarified by ultracentrifugation at 40 000g (rotor T-1270, Thermo Fisher) for one hour with a subsequent filtration through a 0.45 µm sterile filter unit (Sartorius Stedim Biotech).

2.1.2. Purification of HetRV6 RdRp fused to a polyhistidine tag

The purification was performed in the cold room at 4°C using ÄKTA prime chromatography system (Amersham Pharmacia Biotech), which was washed in advance with 1 M NaOH (Riedel-de Haen) for 20 min at 1 ml/min to remove possible ribonuclease (RNase) contamination. Then the system was thoroughly washed with mQ water and HisTrap HP 1 ml column (GE Healthcare) was connected. In chromatographic experiments, the reagents of analytical grade purchased from Sigma-Aldrich were used for the preparation of the buffers. The HisTrap HP column was equilibrated with the buffer A1 (300 mM NaCl, 45 mM imidazole, 50 mM sodium phosphate pH 8.0) followed by the buffer B1 (300 mM NaCl, 300 mM imidazole, 50 mM sodium phosphate pH 8.0) and the buffer A1 again. The clarified bacterial lysate of BL21(DE3)pLysS/His-HetRV6pol cells (see *2.1.1*) was loaded onto the pre-equilibrated column using P1 peristaltic pump (Pharmacia). A linear elution method of 35 column volumes (CV) from 45 mM to 300 mM imidazole at 1 ml/min was applied to elute HetRV6 RdRp. The elution fractions were collected and those corresponding to the peak area were analyzed with sodium dodecyl sulfate polyacrylamide gel electrophoresis (SDS-PAGE). The fractions containing HetRV6 RdRp were combined followed by concentration and buffer exchange with Amicon Ultra-4 centrifugal filter devices (Merck) with molecular weight cut-off (MWCO) of 50 kDa. The elution buffer was exchanged to 50 mM sodium phosphate pH 8.0, 100 mM NaCl, and 10% glycerol.

2.1.3. Purification of native HetRV6 RdRp using dye-ligand affinity chromatography

A set of dye-ligand affinity resins including Cibacron blue 3GA, Reactive brown 10, and Reactive green 19 agarose (Sigma) was tested for possible binding with the tagless HetRV6 RdRp. To this end, a 2 ml of each resin was put into a gravity flow poly-prep chromatography column (Bio-Rad), where it was thoroughly washed with 100 ml mQ water followed by the 10 ml of the buffer A2 (50 mM Tris-HCl pH 8.0, 0.1 mM EDTA). The 3 ml of bacterial lysate was slowly loaded onto the top of the column capped at the bottom. The sample was let to stand for 5 min, after which the bottom cap was removed and flowthrough was collected. The collected flowthrough was re-loaded two more

times. Then the column was washed with 6 ml buffer A2, capped, and 1ml elution buffer B2 containing 50 mM Tris-HCl pH 8.0, 0.1 mM EDTA and 1 M NaCl was added. The column content was incubated 5 min, the cap was removed and the eluate was collected.

2.1.4. Purification of tagless HetRV6 RdRp using a combination of heparin and anion-exchange chromatography

The clarified lysate of IPTG-induced BL21(DE3)pLysS/HetRV6pol expression strain was loaded onto 1 ml HiTrap Heparin HP column (GE Healthcare). The column was subsequently washed with the buffer A3 (50 mM sodium phosphate pH 8.0, 100 mM NaCl, 0.1 mM EDTA) until the detector UV signal baseline stabilized. Then a 35 CV linear gradient elution method from 0 to 1 M NaCl at 1 ml/min flow rate was applied. The 1 ml fractions were collected and analyzed with SDS-PAGE in 16% polyacrylamide gel. The HetRV6 RdRp-containing fractions were diluted 10-fold with mQ water and loaded onto 1 ml HiTrap Q HP anion exchange chromatography column (GE Healthcare), pre-equilibrated with the buffer A3. A linear gradient of 35 CV from 0 M NaCl to 1 M NaCl was applied at 1 ml/min. The fractions containing most of the target protein were collected and loaded onto HiLoad 26/600 Superdex 200 prep grade column (GE Healthcare), pre-equilibrated with the buffer A3. Buffer A3 was also used at the elution step. The fractions containing the HetRV6 RdRp were concentrated with Amicon Ultra-15 centrifugal filter unit (Merck) with MWCO of 30 kDa. The protein concentration was measured using Bradford assay (Bradford, 1976), and, finally, the protein preparation was diluted to 0.4 mg/ml with a storage buffer (62.5% glycerol, 50 mM Hepes-KOH pH 8.0, 0.1 mM EDTA pH 8.0, 0.125% Triton X-100, 100 mM NaCl, 2 mM $MnCl_2$). Homogeneity and identity of the purified polymerase was confirmed by SDS-PAGE in 16% polyacrylamide gel (see *2.3* for details) and western blotting. The expected molecular weight of the expressed protein was calculated using online bioinformatics resource Expasy (SIB Swiss Institute of Bioinformatics, https://web.expasy.org/compute_pi/). For western blot, proteins separated with SDS-PAGE were transferred onto Immobilon P polyvinylidene fluioride membrane (Millipore) in semi-dry electrotransfer device (PHASE). The blocked membrane was probed with primary rabbit polyclonal antibodies raised against HetRV6 RdRp (GeneCust). Anti-rabbit IgG-peroxidase antibodies (Sigma-Aldrich) were used as the secondary antibodies. After application of the enhanced chemiluminecence substrate (Western lightning plus, PerkinElmer), the signal was detected with ChemiDoc imaging system (Bio-Rad).

2.2. Enterokinase cleavage of the polyhistidine tag

The cleavage of a polyhistidine tag was initiated in 50 µl reactions containing enterokinase buffer (2 mM $CaCl_2$, 50 mM NaCl, 20 mM Tris-HCl pH 8.0), 40 µg of the HetRV6 RdRp expressed from pET-32b(+) construct (see *2.1.1*), and 0.05 U, 0.2 U, 0.5 U, 2 U, or 5 U of the enterokinase cleavage enzyme (abm). The reactions were incubated at room temperature or at 4°C with or without 0.5 M urea. After certain periods, the reactions were stopped by adding SDS-PAGE protein loading buffer and analyzed with SDS-PAGE.

2.3. Sodium dodecyl sulfate polyacrylamide gel electrophoresis (SDS-PAGE)

Two type of the SDS-PAGE systems were used: 1) 8×7 cm mini gels (Amerscham Biosciences Mighty small II) served for quick assessment of the protein expression and intermediate purification steps, and 2) 9×8 cm ATTO gels (ATTO Corp) were used for a more accurate assessment of protein purity. Both gels were 16% SDS-PAGE according to (Laemmli, 1970). The samples to be analyzed were mixed with in-house produced SDS-PAGE loading buffer, boiled 3 min and loaded onto the gel. The proteins on mini-gels were analyzed at 200 V and 100 mA for 1 h, whereas ATTO gels were analyzed at 120 V, 60 mA for 3 h. The gels were subsequently stained with Coomassie Brilliant Blue R-250 (Sigma) for 9 min and destained in 10% acetic acid overnight.

2.4. Assay for RNase contamination

To confirm that purified HetRV6 polymerase is RNase-free, 2 µg of enzymatically-produced HetRV6 (+)ssRNA1 (see *2.5*) was incubated with recombinant HetRV6 polymerase in the reaction buffer for 1 h at 37°C. The RNA integrity was verified by agarose gel electrophoresis.

2.5. Production of template (+)ssRNA molecules in vitro

The (+)ssRNA molecules, used as templates in polymerase assays (see *2.6*), were synthesized by *in vitro* transcription with T7 DdRp. The target sequences were amplified in PCR from the plasmids listed in the appendix 2 using corresponding forward primers containing T7 promoter sequences at their 5' ends and reverse primers (primers are listed in the appendix 1). The resulting DNA templates were purified from agarose gel with NucleoSpin Gel and PCR Clean-up kit (Macherey Nagel). The plasmids pEM15 (Makeyev and Bamford, 2000) and pEM19 (Laurila et al., 2002) were digested with *SmaI* restriction enzyme (Fermentas) to prepare templates for the synthesis of phi6 (+)ssRNA designated as Δs^{+}_{13} and Δs^{+}_{HP}, respectively. The digested plasmids were purified with QIAquick PCR purification kit (Qiagen). To produce ssRNA molecules, 200 µl transcription reactions were set up, where 2 µg of selected DNA template was incubated at 37°C with a mixture of four NTPs (5 mM each, Fermentas), 160 U of Ribolock (Thermo Fischer), and 800 U of in-house

produced T7 DdRp in the T7 transcription buffer (120 mM Hepes-KOH pH 7.5, 24 mM $MgCl_2$, 20 mM DTT, 1 mM spermidine). After 2 h of incubation, the RQ1 RNase-free DNase (Promega) was added to remove DNA template. The ssRNAs were extracted with chloroform (Merck) and precipitated with 4 M LiCl (Finnzymes). The pellet was washed with 70% ethanol, dissolved in 400 µl of mQ water and re-precipitated with 0.3 M sodium acetate pH 6.5 and 67% ethanol. The obtained RNA pellet was washed two times with 70% ethanol and dissolved in sterile RNase-free mQ water.

2.6. Polymerase assay

The 20 µl polymerase activity reaction included 50 mM Hepes-KOH (Sigma-Aldrich) pH 7.4, 80 mM ammonium acetate (Merck), 6% (w/v) polyethylene glycol 4000 (Merck), 5 mM $MgCl_2$ (Riedel-de Haen), 1 mM $MnCl_2$ (Sigma-Aldrich), 0.1 mM EDTA (Merck), 0.1% Triton X-100 (Merck), 1 mM of each NTP (Fermentas), 70–140 pM ssRNA template, and 0.8 U/µl RNasin (Promega). For certain indicated reactions, the mixture was supplemented with 0.25 mCi/ml of [α-^{33}P]UTP (PerkinElmer, 3000 Ci/mmol). Reactions were initiated by addition of 0.8–1.2 µM of the in-house produced HetRV6 RdRp. In the control reactions, enzyme was replaced with an equal volume of the RdRp storage buffer (see *2.1.4*). After indicated time, the reactions were stopped by addition 2×U loading dye [8 M urea, 10 mM EDTA, 0.2% SDS, 6% (v/v) glycerol, 0.05% bromophenol blue and 0.05% xylene cyanol FF] and analyzed with native agarose gel electrophoresis (see *2.9*). To calculate the reaction polymerization rate (nt/min), a number of nucleotides in a template ssRNA was divided by the time of the incubation (min) required for a full-length dsRNA product to appear.

2.7. TNTase assay

The TNTase activity was measured under conditions similar to polymerase assay in the presence of 0.3 µM UTP supplemented with 0.25 mCi/mL of [α-33P]-UTP (PerkinElmer, 3000 Ci/mmol). The other three NTPs were not included in the reaction mixture. Reactions were initiated by addition of the HetRV6 RdRp or in-house prepared phi6 RdRp (Makeyev and Bamford, 2000) to a final concentration of 1 µM. In the control reactions, the RdRp storage buffer was added instead of the enzymes. The mixtures were incubated 90 min at 30°C.

2.8. LiCl fractionation of RNA molecules

After polymerase assay (see *2.6*), molecules of ssRNA were precipitated with 2 M LiCl (Merck) at -20°C for 30 min followed by 20 min centrifugation at 13,000×*g* and 4°C. The dsRNA was precipitated from the supernatant by 4 M LiCl followed by the incubation and centrifugation

steps as described above (Diaz-Ruiz and Kaper, 1978). The dsRNA pellet was washed twice with 70% ethanol and dissolved in nuclease-free water.

2.9. Analysis of RNA with agarose gel electrophoresis and autoradiography

The ss- and dsRNA molecules produced in the current study, were analyzed in 1% native agarose gel using Tris/borate/EDTA (TBE) buffer (50 mM Tris-borate pH 8.3, 1 mM EDTA). The RNA separation was performed at 5 V/cm, and RNA molecules were visualized by means of intercalating dye ethidium bromide. The gels were photographed, dried and exposed against the imaging plates (Fujifilm), which were subsequently scanned with Typhoon TRIO Imager (GE Healthcare).

3. RESULTS

3.1. HetRV6 polymerase is expressed as a soluble and active in vitro protein

3.1.1. Expression and purification of polyhistidine-tagged HetRV6 RdRp

In order to get a fast initial confirmation that HetRV6 RdRp can be expressed *in vitro* as a soluble and active protein, a pET-32b(+)-based construct generating the polymerase fused to His-tag at the N-terminus was prepared and transformed into the *E. coli* expression strain. The resulting BL21(DE3)pLysS/His-HetRV6pol cells were used to induce the expression of the recombinant HetRV6 RdRp with His-tag. The same *E. coli* strain transformed with an empty pET32b(+) vector was used as the control. The analysis of the clarified bacterial lysates with SDS-PAGE demonstrated that recombinant HetRV6 RdRp with His tag was expressed to a high level as a soluble protein from the corresponding construct (Figure 1). From the empty vector, about 20 kDa protein was expressed, but no significant protein expression was detected in the size range of HetRV6 RdRp (Figure 1).

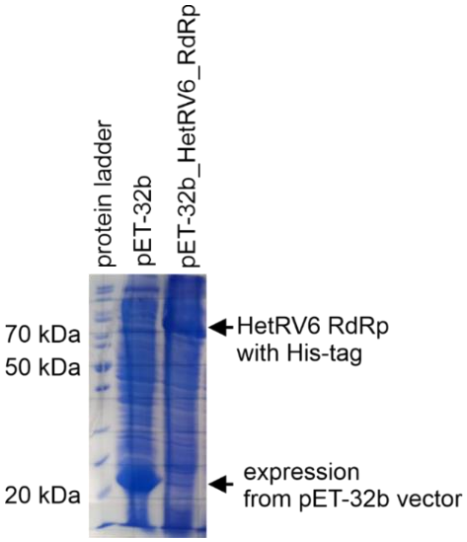

Figure 1. **Expression of the polyhistidine-tagged HetRV6 RdRp**. The *E. coli* strain BL21(DE3)pLysS was transformed with pET-32b(+) vector containing the polymerase sequence or empty vector, to serve as a control. After IPTG-induced protein expression at 17°C for 18 h, the cells were lysed with ultrasound; the lysates were clarified and loaded onto 16% SDS-PAGE polyacrylamide gel to confirm the expression of the soluble HetRV6 RdRp. PageRuler unstained protein ladder (Thermo Fisher) was used to confirm the size of the expressed proteins.

The clarified bacterial lysates were subjected to Immobilized Metal Affinity Chromatography (IMAC). The fractions of the control sample analyzed on SDS-PAGE gels showed a single protein of about 20 kDa without visible contaminations. However, fractions collected during HetRV6 RdRp purification contained multiple proteins of smaller size, which could originate from uncontrolled HetRV6 RdRp degradation under the applied purification conditions (Figure 2).

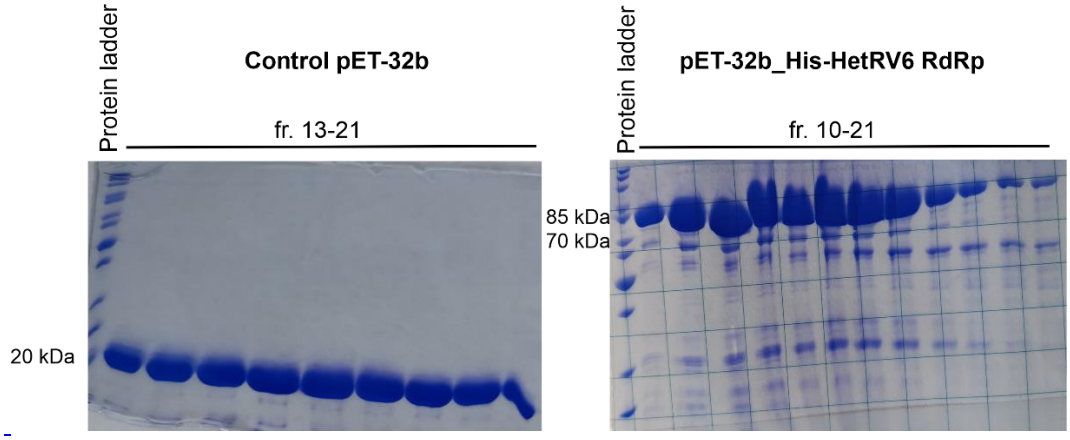

Figure 2. Purification of bacterial lysates using IMAC. The clarified bacterial lysates from control strain (left) and HetRV6 RdRp expression strain (right) were loaded onto HisTrap HP column, the peak fractions were collected and analyzed in 16% SDS-PAGE gel. PageRuler unstained protein ladder (Thermo Fisher) was used to confirm the size of the expressed proteins.

The fractions 11–17 after HetRV6 RdRp purification were combined for the concentration and buffer exchange with Amicon Ultra centrifugal filter devices. Then polymerase assays containing 0.5, 1 and 3 µl of the HetRV6 RdRp preparation were set up to check for activity (Figure 3). I used two heterologous (+)ssRNA templates of 710 bp (Δs^+) and 2948 bp (s^+) derived from the S segment of bacteriophage phi6 genome (please see *2.5* and appendices for more details). Both templates carried the same nucleotide sequence at the 3' end, where a nascent RNA synthesis starts, and both appeared to be suitable templates for HetRV6 RdRp despite a significant size difference (Figure 3).

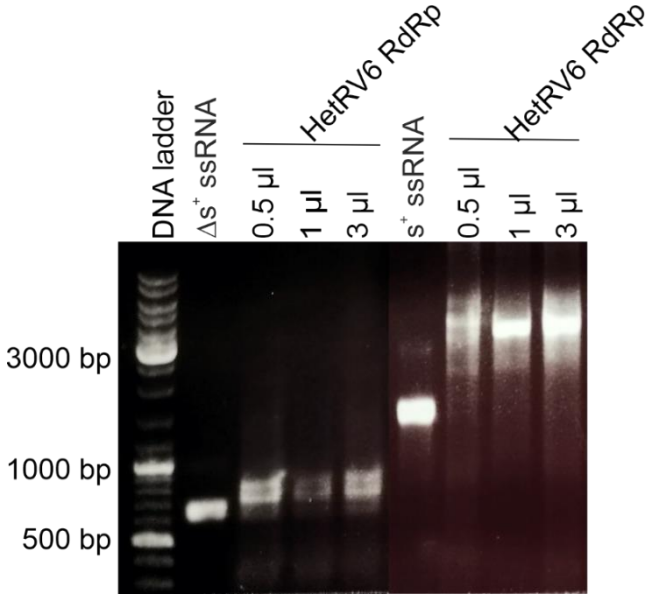

Figure 3. Polymerase activity of the purified HetRV6 RdRp with polyhistidine tag. The IMAC fractions containing HetRV6 RdRp were combined, concentrated and put into the buffer without imidazole. Full-length (+)ssRNA of the bacteriophage phi6 (s^+) and its truncated version (Δs^+) were used as templates for the replication reactions containing increasing amounts of the HetRV6 RdRp preparation. The template ssRNAs Δs^+ and s^+ are also shown on the gel. The amounts of HetRV6 RdRp preparation added to the template is shown on top of the gel. GeneRuler DNA ladder mix was used to confirm the size of the nucleic acids.

Together with a polyhistidine tag, a recombinant HetRV6 RdRp expressed from the pET-32b(+) vector contained about 150 extra amino acids at the N-terminus originating from the expression region of the vector (see appendix 3 for clarification), which potentially could interfere with the protein folding and affect some of its enzymatic activities. Therefore, I tried to remove this sequence with enterokinase cleavage (Figure 4). The cleavage was performed both at room temperature and at 4°C. The samples were analyzed after 2 h, 6 h and 24 h after the beginning of cleavage. The best results were achieved after 2–4 h of incubation at 4°C in the presence of 2–5 units of enterokinase and 0.5 M urea, when the N-terminal sequence was removed from almost half of the input protein (Figure 4A and C). Nevertheless, the cleavage was, in general, inefficient, leading to unspecific protein degradation after only 2 h of incubation at room temperature, and at later time points also at 4°C (Figure 4B, C, E).

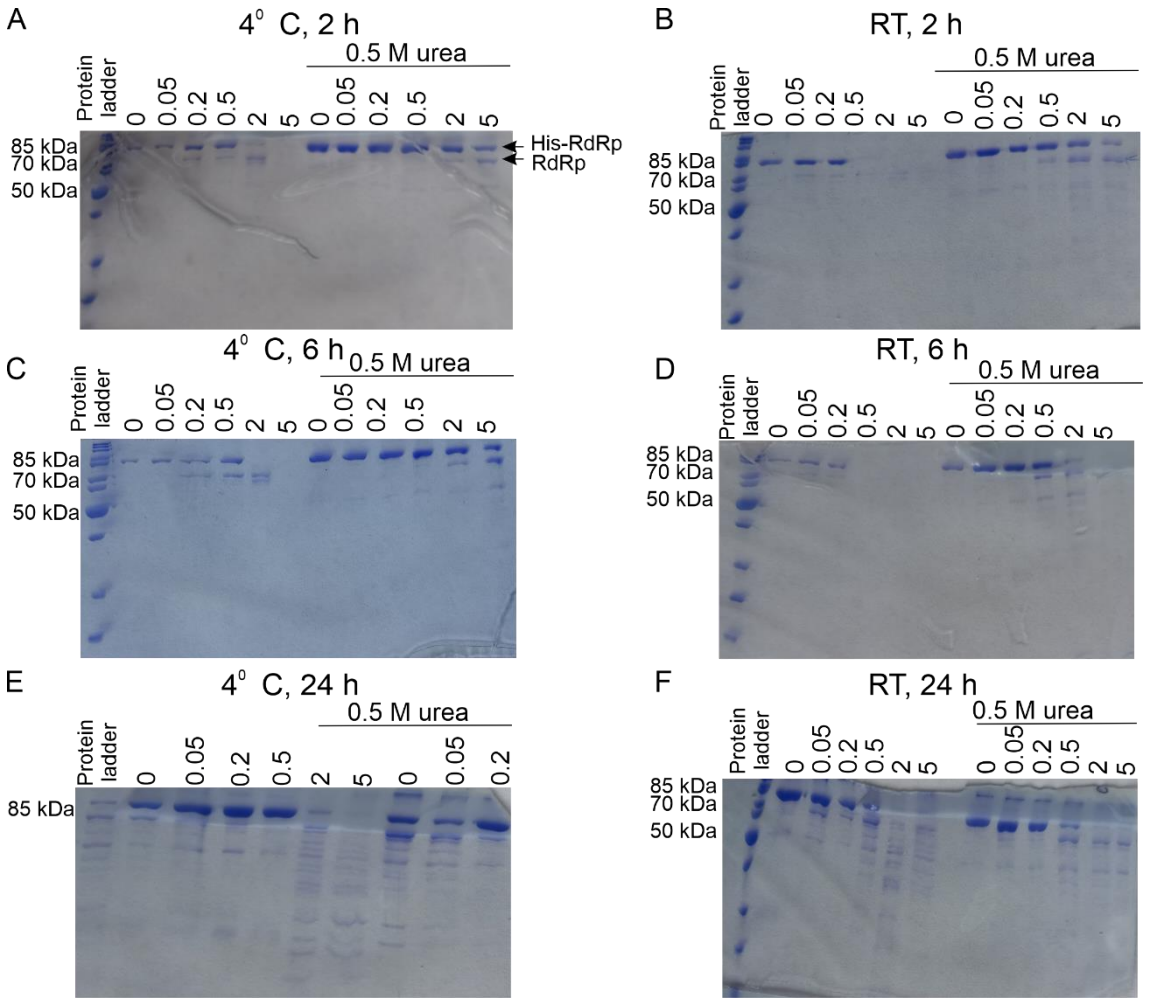

Figure 4. Enterokinase cleavage of the N-terminal extra sequence from HetRV6 RdRp containing polyhistidine tag. Purified HetRV6 RdRp was incubated with variable amounts of enterokinase to cleave off the extra 150 amino acids at the N-terminus. The incubation was carried out at room temperature (RT) and 4°C with or without 0.5 M urea. The amounts of enterokinase (U in 50 µl reaction) are indicated on the top of SDS-PAGE gels.

I tried to optimize the incubation time with enterokinase to achieve more efficient cleavage of the non-specific N-terminal sequence from the HetRV6 RdRp. To this end, I incubated the purified protein in 50 µl reaction with either 0.5 U or 2 U of enterokinase at 4°C for 3, 5, 6, 7 or 24 h. Similar to the previous experiments, I achieved only ~50% cleavage after 3 h of incubation using 0.5 U of enterokinase. The increase in either enerokinase amount or incubation time resulted only in abundant non-specific cleavage of the polymerase, but not in the improved target-specific cleavage of the N-terminal sequence (Figure 5).

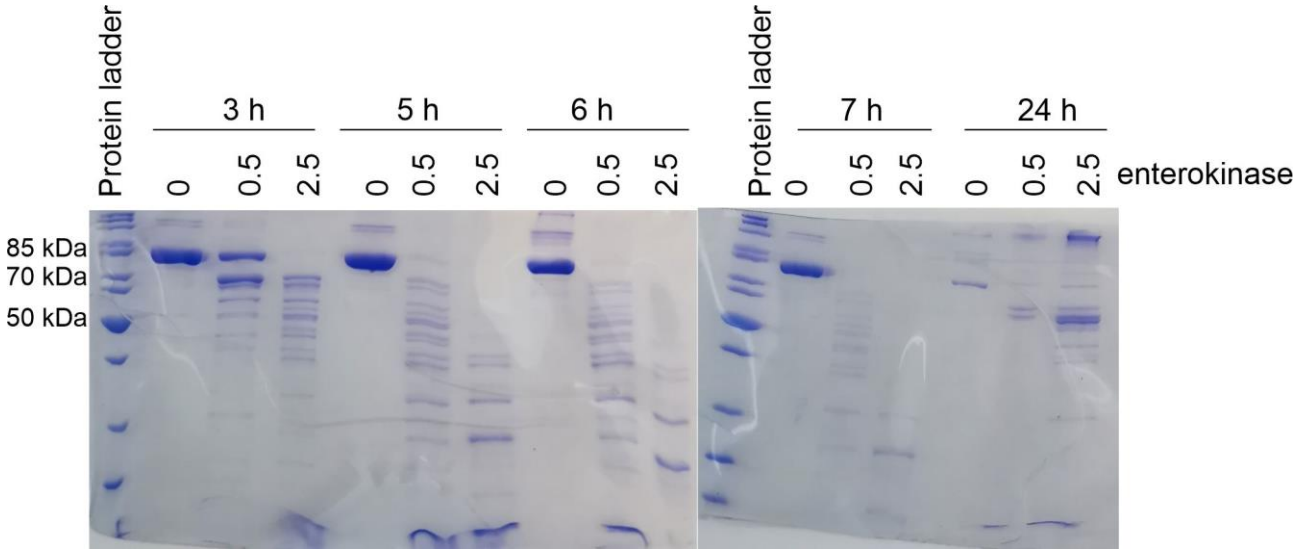

Figure 5. Enterokinase cleavage of the N-terminal polyhistidine tag from HetRV6 RdRp construct. Purified HetRV6 RdRp was incubated with variable amounts of enterokinase to cleave off the extra 150 amino acids at the N-terminus. The incubation was carried out at 4°C. The amounts of enterokinase (U in 50 µl reaction) are indicated on the top of SDS-PAGE gels.

Thus, after performing the initial experiments it became clear that recombinant HetRV6 RdRp can be expressed and purified from bacterial cells as a soluble protein, which is active *in vitro* and catalyzes dsRNA synthesis on heterologous templates of variable size in a primer-independent manner. However, for unbiased biochemical studies and possible future crystallization experiments, the non-specific N-terminal sequence should be removed from the protein. It was impossible to cleave off this sequence efficiently with enterokinase. Therefore, at the next step I expressed HetRV6 RdRp without any tags and developed a chromatographic method for its purification.

3.1.2. Purification of the recombinant HetRV6 RdRp without any tags

The recombinant HetRV6 RdRp that did not contain any additional sequences was expressed in *E. coli* cells similarly to its counterpart with a polyhistidine tag using the expression plasmid pET-28a(+) containing a cDNA copy of the HetRV6 gene (see *2.1.1*). The tagless polymerase was expressed in high amounts as a soluble protein (Figure 6).

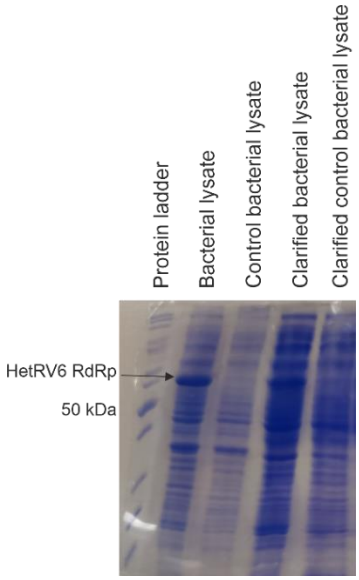

Figure 6. Expression of tagless HetRV6 RdRp. The tagless HetRV6 RdRp was expressed from pET-28a(+) vector in *E. coli* bacterial cells. The control *E. coli* cells were transformed with an empty expression vector. The bacterial lysates were clarified by high-speed centrifugation followed by filtration.

To purify tagless HetRV6 RdRp, I tested resins used for dye-ligand affinity chromatography such as Cibacron blue 3GA, Reactive brown 10 and Reactive green 19 agarose. However, the polymerase did not bind significantly to any of them and eluted in the flowthrough or during the washing step (Figure 7).

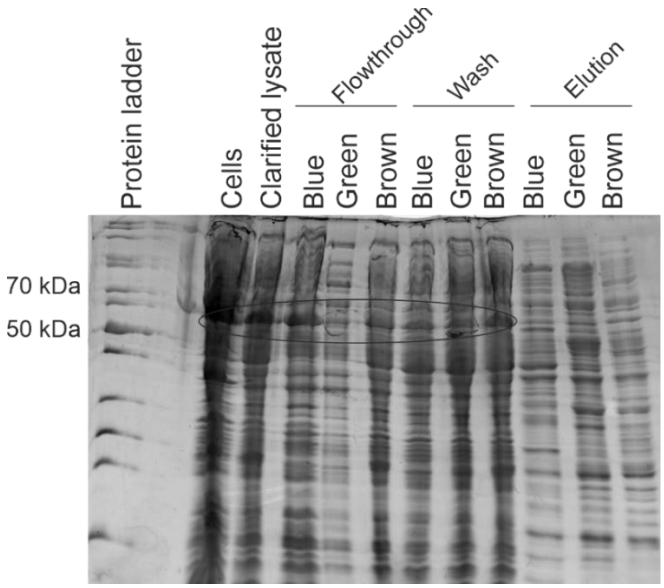

Figure 7. Binding of HetRV6 RdRp to affinity dye ligands. The tagless HetRV6 RdRp was expressed from pET-28a(+) in *E. coli* cells (Cells), which were disrupted by sonication and the lysate was clarified by high-speed centrifugation and filtration (Clarified lysate). The clarified lysate was loaded onto gravity flow columns containing either Cibacron blue 3GA (Blue), Reactive green 19 (Green) or Reactive brown 10 (Brown) agarose. The flowthrough, wash and elution fractions were analyzed by SDS-PAGE. The position of the recombinant HetRV6 RdRp is marked with an eclipse.

After unsuccessful attempts to purify HetRV6 RdRp with dye affinity chromatography, I decided to use heparin column as an initial purification step. The SDS-PAGE showed that HetRV6 RdRp binds efficiently to the Heparin column (Figure 8). The optimal results were obtained when purification of the HetRV6 RdRp on HiTrap Heparin HP column was followed by the HiTrap Q HP anion exchange column (Figure 8 and 9). Size exclusion chromatography (SEC) was used as a final polishing step (Figure 10).

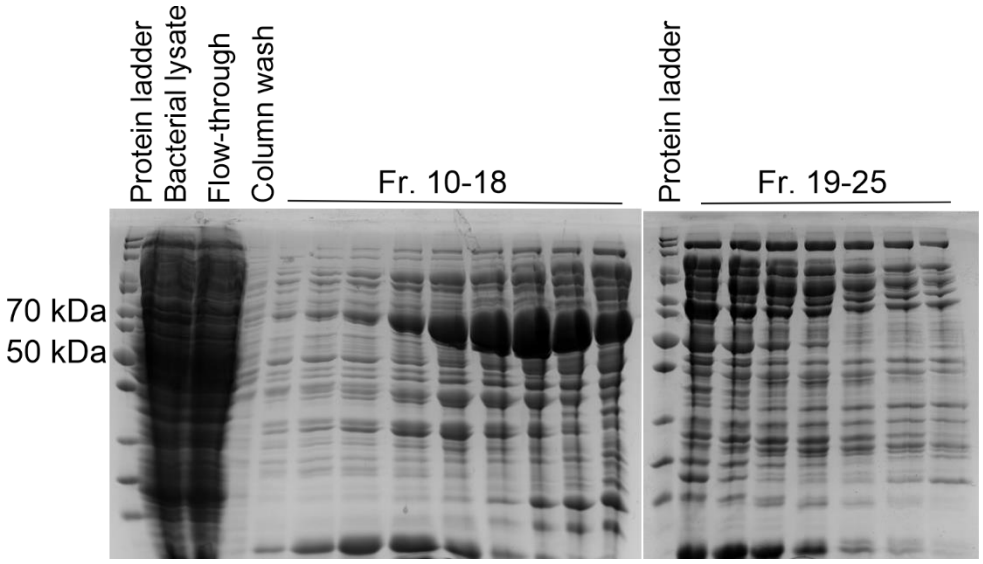

Figure 8. **Purification of tagless HetRV6 RdRp by heparin affinity chromatography**. The clarified bacterial lysate after protein expression was loaded onto 1 ml HiTrap Heparin HP column followed by the column wash and elution with a linear gradient of 35 column volumes from 0 mM NaCl to 1 M NaCl at 1 ml/min. Fractions of 1 ml were collected and those corresponding to the peak area were analyzed on 16% polyacrylamide gel.

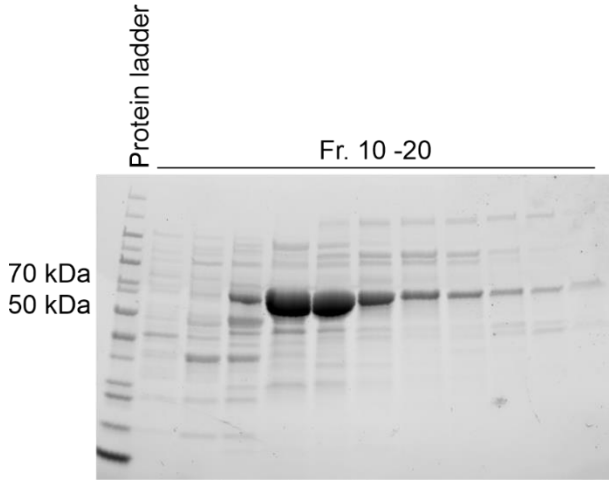

Figure 9. **Purification of the recombinant HetRV6 RdRp by ion-exchange chromatography.** Fractions from the heparin column containing HetRV6 RdRp were combined, diluted 10-fold and loaded onto Q column followed by the elution with a linear gradient of 35 column volumes from 0 mM NaCl to 1 M NaCl at 1 ml/min. Fractions of 1 ml fractions were collected and those corresponding to the peak area were analyzed onto 16% polyacrylamide gel.

HetRV6 RdRp eluted from the heparin column at ~400 mM NaCl (Figure 8), and from the Q anion exchange column at ~300 mM NaCl (Figure 9). The purity and identity of the HetRV6 RdRp was conclusively indicated with SEC, SDS-PAGE and western blotting (Figure 10). The protein eluted as a monomer from the SEC column (Levanova et al., 2021), and the experimentally observed molecular weight of the protein corresponded to the theoretically calculated value of 69.3 kDa (see *2.1.4* for details).

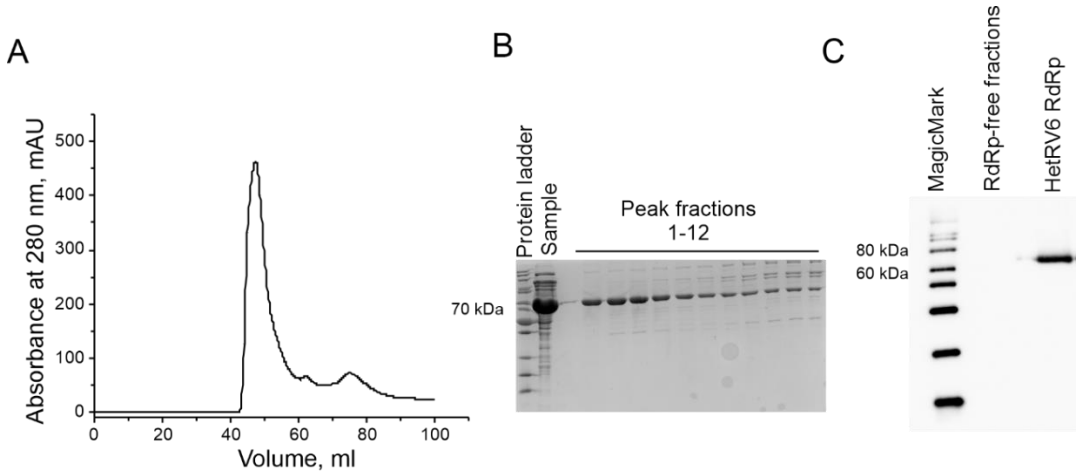

Figure 10. **Size-exclusion chromatography (SEC) and verification of HetRV6 RdRp identity and purity**. (A) Chromatogram showing elution profile of the HetRV6 RdRp after HiLoad 26/600 Superdex 200 prep grade column (GE Healthcare). (B) Analysis of the SEC fractions with 16% SDS-PAGE. The input sample is shown in the second well of the gel. The peak fraction 1 corresponds to the elution volume of 42 ml. (C) Western blotting with rabbit anti-HetRV6 RdRp polyclonal antibodies verified the identity of HetRV6 RdRp (modified from Levanova et al., 2021).

The activity of HetRV6 RdRp polymerase fractions was initially tested under the conditions described for the polymerase of a dsRNA virus phi6 (Makeyev and Bamford, 2000). As a template, a full-length native (+)ssRNA1 produced from the cDNA of the dsRNA1 genome segment of HetRV6 was used (Figure 11).

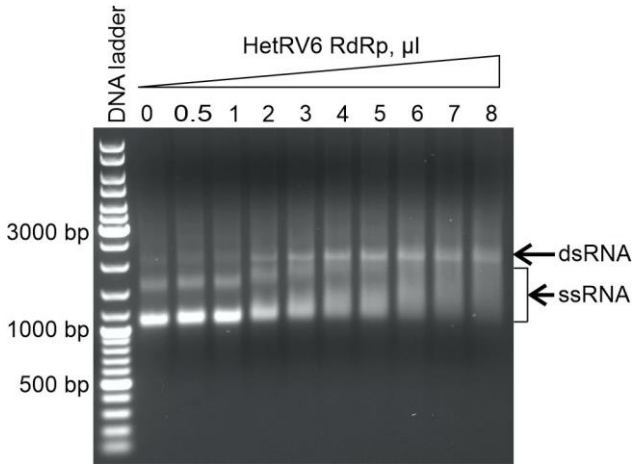

Figure 11. **In vitro polymerase activity of the HetRV6 RdRp on the native template**. The polymerase reactions with increasing volumes of the HetRV6 RdRp-containing fractions after SEC. The native HetRV6 (+)ssRNA1 was used as a template.

The purified enzyme was active and full-length dsRNA was observed on the gel for the reactions, where 2–8 µl SEC fractions were used (Figure 11). The SEC fractions were concentrated, put into the storage buffer with glycerol and incubated with ssRNA at 37°C. No visible degradation of RNA was detected after the incubation with the purified HetRV6 RdRp (Figure 12), which confirmed that it is free of RNases.

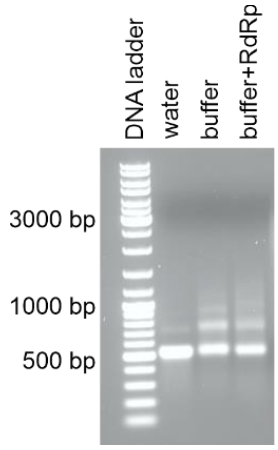

Figure 12. RNase contamination assay with HetRV6 RdRp. A HetRV6 (+)ssRNA1 was incubated with water, polymerase storage buffer or buffer with HetRV6 RdRp at 37°C for 1 h.

3.2. Optimization of the reaction buffer composition

To dissect the role of critical buffer components on polymerase activity and determine their optimal content in the reaction mixture, I set up polymerase assays, in which the concentration of a single reagent was systematically changed, while the rest remained constant (please see *2.6* for the basic composition of the reaction). When the incubation time was over, the ssRNA and dsRNA were fractionated by LiCl precipitation (see *2.8*) and the amount of dsRNA in the sample was determined spectrophotometrically. The highest activity of the HetRV6 RdRp was observed in Hepes-KOH buffer at pH 8.0. Tris-HCl buffer substantially inhibited the replicase activity of the enzyme. This Tris-HCl intolerance distinguishes the enzyme from the previously characterized phi6 RdRp (Makeyev and Bamford, 2000). Ammonium ions in the concentration of 40 mM and 1–5 mM Mg^{2+} ions enhanced the dsRNA production, while Mn^{2+} ions in the concentration 1–2 mM were indispensable for the RdRp activity (Figure 13).

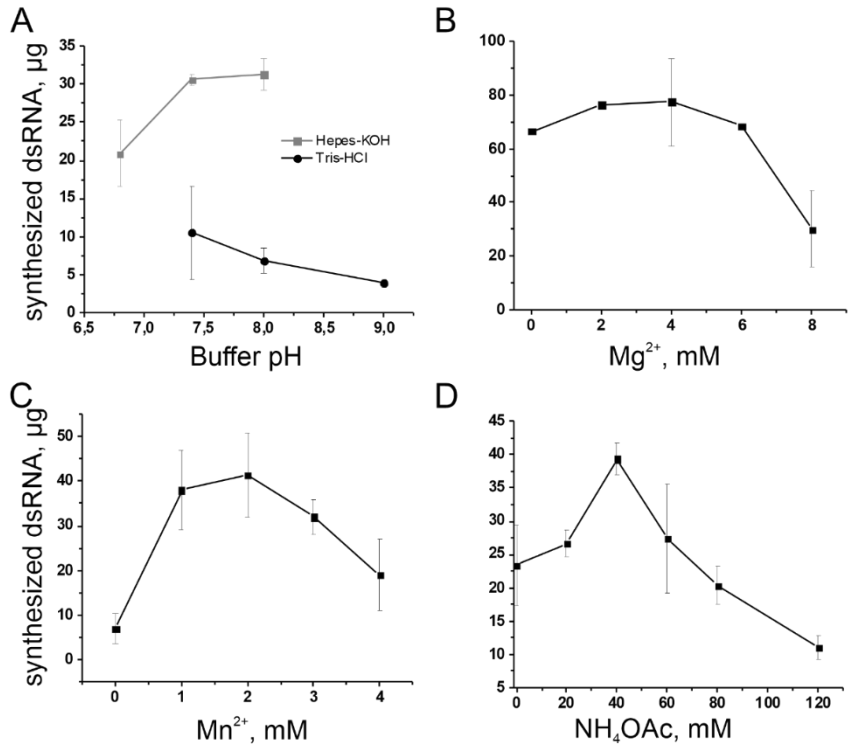

Figure 13. Optimization of the reaction conditions for HetRV6 RdRp. The polymerase reactions were set up with the native HetRV6 (+)ssRNA1 template. The influence of one reaction component at a time was studied, while the others remained unchangeable. (A) Impact of the buffer and its pH on the dsRNA production; (B) Mg^{2+} ions and reaction efficiency; (C) Role of Mn^{2+} ions in the dsRNA production; (D) Optimal amount of ammonium acetate (NH_4OAc). The figure is modified from Levanova et al., 2021.

3.3. Influence of the incubation temperature on the polymerization rate of the HetRV6 RdRp

To select the optimal incubation temperature for nucleotide polymerization, I studied the kinetics of polymerase reaction at 24°C (room temperature), 30°C, and 37°C (Figure 14) under optimized buffer conditions. The enzyme was active at all three temperatures. However, as expected, the temperature increase resulted in significant rise in the polymerization rate. Thus, full-length product was detected after 180 min at 24°C, after 90 min at 30°C and after 60 min at 37°C (Figure 14). The calculated polymerization rate was 2-fold and 3-fold higher at 30°C and 37°C, respectively, compared to that observed at 24°C (Table 1). Furthermore, after 180 min incubation at 24°C only a tiny fraction of ssRNA template was replicated to dsRNA and the reaction should be incubated about 300 min to get a reasonable amount of dsRNA (Figure 14A). Typically, replication rate and efficiency of dsRNA synthesis, as judged by the intensity of dsRNA bands, were the largest at 37°C. However, this temperature is far from that at which HetRV6 RdRp operates naturally. Therefore, I selected 30°C as an optimal temperature for further experiments.

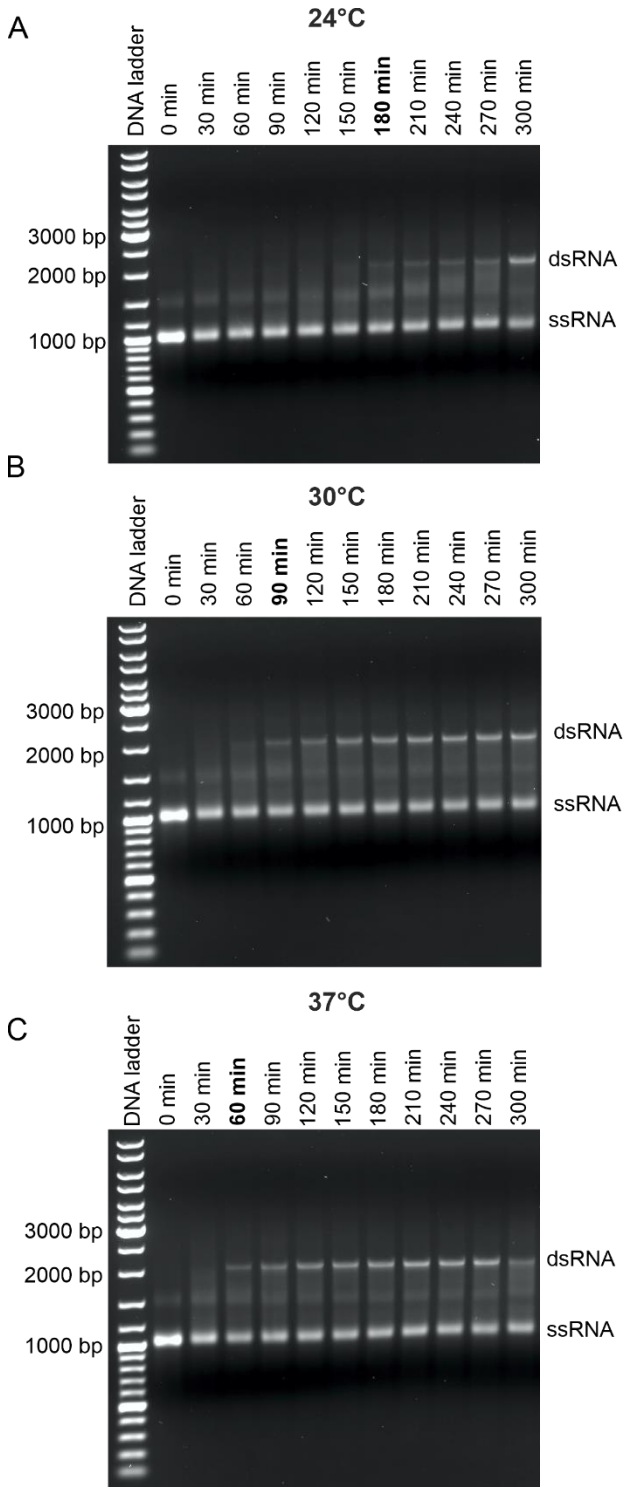

Figure 14. **Optimization of the reaction temperature for the HetRV6 RdRp.** 100 µl polymerase reaction was set up at 24°C (A), 30°C (B), and 37°C (C). At regular time intervals, an aliquot of 6.5 µl was taken for the analysis in 0.8% native agarose gel. Time point at which full-length dsRNA was detected is in bold. Modified from Levanova et al., 2021.

Table 1. Polymerization rate of the HetRV6 RdRp-catalyzed reaction at different incubation temperatures

Temperature	24°C	30°C	37°C
Polymerization rate	11 nt/min	23 nt/min	34 nt/min

3.4. Impact of NTP concentration on the polymerization rate of HetRV6 RdRp

To understand how NTP concentration influences the HetRV6 RdRp-catalyzed replication, I set up the polymerase reactions under the optimal conditions described in chapters *3.2* and *3.3* with variable NTP concentrations. In literature, NTPs in the final concentration of 0.2 mM and 1 mM are commonly applied in polymerase assays (e.g., Makeyev and Bamford, 2000). The native HetRV6 (+)ssRNA1 template has a 5'-…GCUG-3' sequence at the 3' end. Thus, the first two nucleotides to be included in the nascent strand are cytidylate (CMP) and adenylate (AMP), which I used in excess for certain reactions (Figure 15).

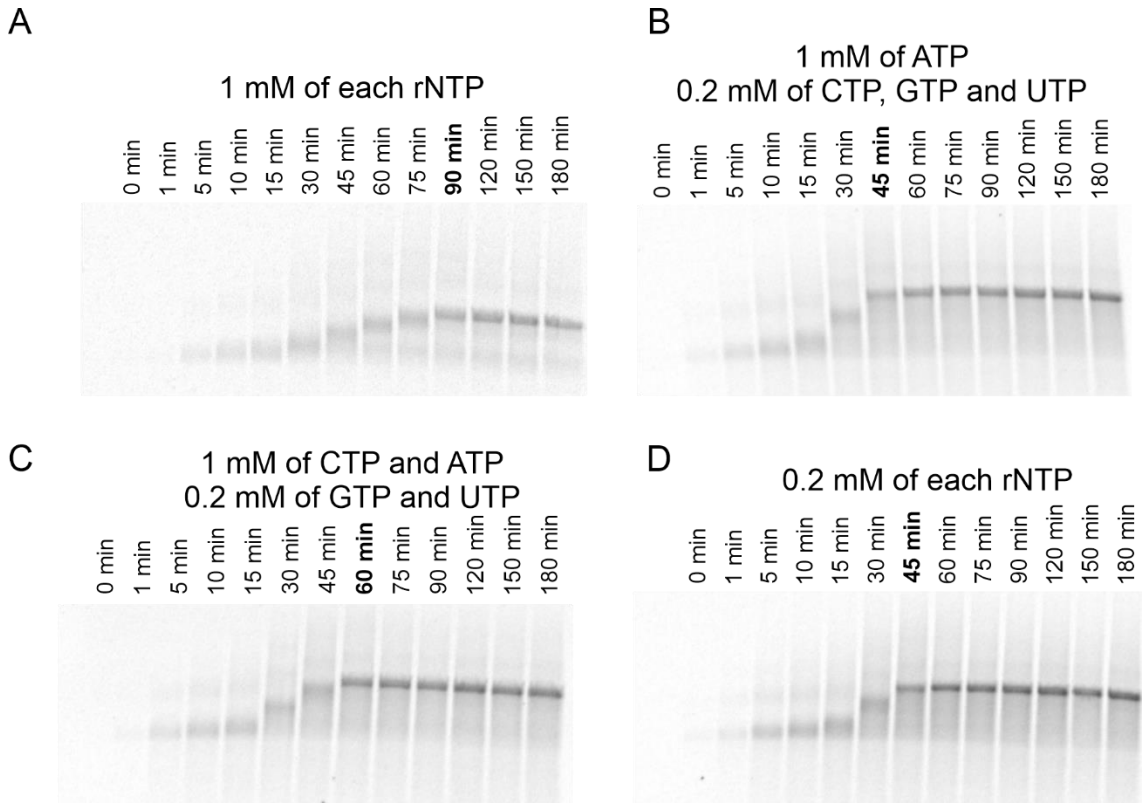

Figure 15. **Impact of NTP concentration on the kinetics of polymerization.** The polymerase assays were set up using [α-^{33}P]UTP under optimal conditions described in *3.2* and *3.3* with the native HetRV6 (+)ssRNA1 as a template and incubated for 3 h at 30°C. At the indicated time points, aliquots of the reaction were taken for the analysis in native agarose gel following by autoradiography. The autoradiograms of the gels are presented. The time points, when the full-length dsRNA can be detected, are shown in bold.

The fastest kinetics for NTP incorporation was observed when all four NTPs were used in the polymerase assay at the concentration of 0.2 mM or only ATP was present at a higher 1 mM concentration (Figure 15, Table 2). With the increase of equimolar NTP concentration to 1 mM, the polymerization rate decreased 2-fold (Table 2). When the starting NTPs (ATP and CTP) were present in the reaction mixture at 1 mM, while GTP and UTP were kept at 0.2 mM, the polymerization rate was between the highest and the lowest ones observed (Table 2).

Table 2. Influence of NTP concentration on the polymerization rate

NTP concentration	1 mM A,C,G,U[1]	1 mM A+ C, 0.2 mM G+U	1 mM A, 0.2 mM C,G,U	0.2 mM A,C,G,U
Polymerization rate	23 nt/min	34 nt/min	46 nt/min	46 nt/min

[1]A – ATP, C – CTP, G – GTP, U – UTP

3.5. HetRV6 performs dsRNA replication on heterologous templates

In the chapter *3.1.1,* I showed that HetRV6 RdRp carrying polyhistidine tag at its N-terminus was capable of replicating heterologous ssRNA templates originated from the bacteriophage phi6 (Figure 3). To confirm that recombinant HetRV6 RdRp without extra amino acid sequences can utilize heterologous (+)ssRNA templates, I produced by *in vitro* transcription a number of heterologous templates of variable length and sequences (please see appendices 1 and 2 for details). The native template HetRV6 (+)ssRNA1 was efficiently replicated, while the RNA synthesis productivity was variable on heterologous templates (Figure 16). All the derivatives from the phi6 Δs^+ ssRNA were suitable templates for the HetRV6 RdRp However, the enzyme was not fully processive on (+)ssRNA2 from a picobirnavirus (PBV). Furthermore, dsRNA molecules were hardly synthesized on the luciferase (+)ssRNA (luc_4) containing two AMPs at the very 3' end (Figure 16). The other luciferase templates were replicated to some extent. (Figure 16).

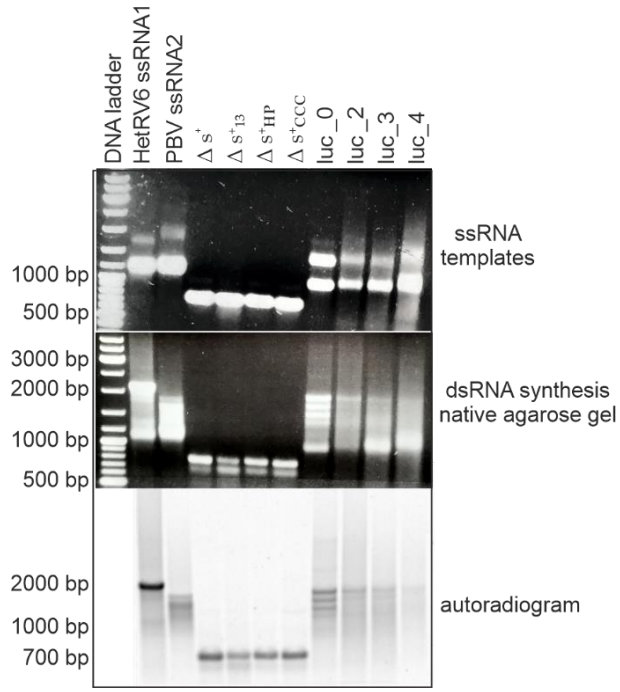

Figure 16. **HetRV6 RdRp-catalyzed dsRNA synthesis on heterologous templates.** The polymerase assay under optimal conditions contained native HetRV6 (+)ssRNA1 or heterologous templates with variable 3' ends shown on the uppermost gel (please see appendix 2 for details). The reaction products were analyzed by native gel agarose electrophoresis following by autoradiography (intermediate and bottom picture, respectively).

3.6. HetRV6 RdRp has terminal nucleotidyl transferase (TNTase) activity

To examine if HetRV6 RdRp can catalyze template-independent nucleotide addition to the 3'-end of RNA molecules, i.e. terminal nucleotidyl transfer (Poranen et al., 2008a), I set up polymerase assays where only a single UTP was present. Similar to phi6 RdRp, for which TNTase activity was extensively studied (Poranen et al., 2008a), HetRV6 RdRp catalyzed addition of an [α-33P]-UTP to the ssRNA templates (Figure 17).

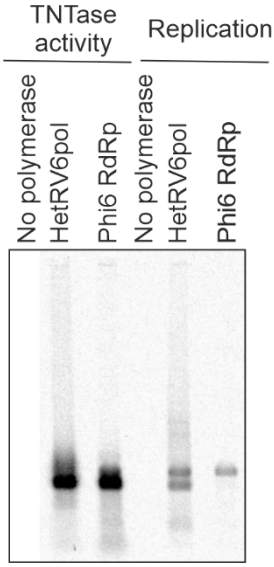

Figure 17. **TNTase activity of HetRV6 RdRp.** Δs^+ ssRNA was used as a template in TNTase and polymerase assays catalyzed either by phi6 or HetRV6 RdRp. After incubation the reactions were analyzed by native agarose gel electrophoresis and autoradiogram of the gel shows label incorporation from [α-^{33}P]-UTP.

4. DISCUSSION

In the present study, I expressed a recombinant HetRV6 polymerase as a soluble protein in bacterial cells and developed a method for its purification, which kept the enzyme RNase-free and active. Enzymatically active recombinant viral RdRps subunits have been previously obtained for (+)ssRNA viruses such as picornaviruses (Ferrer-Orta et al., 2015) and flaviviruses (Duan et al., 2019), some (-)ssRNA viruses [vesicular stomatitis virus (Morin et al., 2012)] and dsRNA viruses [phi6 and some other cystoviruses (Makeyev and Bamford, 2000; Yang et al., 2001), human picobirnavirus (Collier at al,, 2016), infectious pancreatic necrosis virus (Graham et al., 2011)]. However, isolated viral polymerase subunits are not necessarily active *in vitro*. Thus, the ß-subunit, RdRp from the (+)ssRNA bacteriophage Qß, requires additional host factors to assemble an active replicase complex (Takeshita and Tomita, 2012). Furthermore, most viral RdRp subunits that demonstrated some activity *in vitro* are not fully processive, even on the native templates.

My work started with the cloning of the DNA insert representing a full-length copy of the HetRV6 RdRp gene into an expression vector pET-32b(+). The optimal expression temperature

appeared to be 17°C, which extended time of expression to 18–20 h, but allowed to obtain substantial amounts of a soluble polymerase, which were easily detectable by SDS-PAGE (Figure 1 and 6).

Protein purification is often achieved by affinity chromatography via expression of a specific tag fused to a protein of interest. Therefore, initially the protein was expressed with a polyhistidine (6×His) tag and could be purified with IMAC, for which I used HisTrap HP column packed with precharged Ni-Sepharose. The control purification of the small product expressed from the expression vector pET-32b(+) provided a ~20 kDa protein of high purity. On the contrary, HetRV6 RdRp purified on HisTrap HP column contained multiple proteins of smaller size (Figure 2), which might indicate uncontrollable degradation of the polymerase under purification conditions. Furthermore, the performance of IMAC columns can be variable and additional purification steps might be sometimes needed to achieve a pure protein (Riguero et al., 2020). Thus, all the proteins of smaller size were efficiently removed from the HetRV6 RdRp with Amicon filter device (Figure 4 and 5, control bands). The polyhistidine tag could be left on the protein, but it can potentially interfere with certain experiments (Shahravan et al., 2008). Therefore, I decided to make use of the consensus enterokinase recognition sequence (DDDDK) engineered between the desired protein and the N-terminal tag sequence (appendix 3), and applied different amounts of enterokinase and variable incubation times at two different temperatures (4°C and 24°C) to cleave out the N-terminal tag. However, it was not possible to achieve a significant cleavage specificity at the consensus recognition sequence for enterokinase. Any attempt to increase an enzyme amount or incubation time resulted in substantial non-specific protein cleavage rather than in increase of the amounts of the tagless protein (Figure 4 and 5). There are published reports confirming that enterokinase does not exhibit high stringent sequence specificity (Liew et al., 2005; Shahravan et al., 2008). Therefore, I re-cloned the HetRV6 RdRp cDNA into pET-28a(+) vector to get a protein without any extra sequences.

As the first step of the native HetRV6 RdRp purification, I decided to use dye-ligand affinity chromatography since this approach was successfully implemented as the first step in the purification of the recombinant RdRp from bacteriophage phi6 (Makeyev and Bamford, 2000). The dye-ligand affinity chromatography is based on the high affinity of immobilized dyes for many proteins (Stellwagen, 2001). It is fast, cost-effective and versatile method, which is potentially applicable even for the purification of crude bacterial lysates. In my experiments, I applied an approach described by (Stellwagen, 2001), when a small volume of clarified bacterial lysate was loaded onto a series of small gravity flow columns, each containing a certain immobilized dye, Cibacron blue 3GA, Reactive green 19 or Reactive brown 10. However, neither of the dye ligands had affinity to the HetRV6 RdRp (Figure 7).

At the next stage, I used affinity chromatography based on heparin, which is a polysaccharide belonging to the family of glycosaminoglycans. Heparin interacts with a wide range of biomolecules, including nucleic acid-binding proteins (Bolten et al., 2018; Staby et al., 2005). Heparin affinity chromatography was used to purify RNA polymerase from *E. coli* (Sternbach et al., 1975) and a recombinant RdRp from the human picobirnavirus (Collier et al., 2016). The heparin affinity chromatography is very straightforward since it does not require any affinity tags on the target protein and the heparin-binding domains of different proteins are typically easily accessible (Bolten et al., 2018). Heparin acts as an analogue of nucleic acids and shows a stoichiometric binding affinity for nucleic acid proteins (Singh and Jones, 1984). Since heparin contains anionic sulphate groups, it can also serve as a cation exchanger (Xiong et al., 2008). However, I believe that the separation of HetRV6 RdRp on heparin agarose is based on affinity rather than ion exchange chromatography. The calculated pI of the HetRV6 RdRp is 5.62, which means that under the separation conditions in the buffer with pH 8.0, the surface of the protein is predominantly negatively charged and repulsive forces might occur between the protein and the column matrix. Nevertheless, I observed efficient binding of the HetRV6 RdRp to the heparin column with its subsequent elution at the increased ionic strength (Figure 8). Since heparin binds many different proteins, it is not possible to purify HetRV6 RdRp from the bacterial lysate in a single step. Therefore, the protein purification of heparin column was followed by the anion exchange chromatography using strong anion exchange Q column. The use of heparin-agarose rather than ion exchange chromatography as the first purification step has certain advantages. Thus, the heparin agarose has a very high binding capacity allowing using relatively small column bed volumes and, hence, eluting the enzyme in very small volumes. Furthermore, most bacterial nucleases potentially present in the lysate either do not bind to heparin agarose or elute at very low ionic strength (Bickle et al., 1977).

I need to mention, that the recombinant tagless HetRV6 RdRp enzyme had some issues with the stability and became inactive after approximately 6 months of storage at -20°C (the activity of the His-tagged protein was not monitored). As one potential solution to the stability problem, a bovine serum albumin can be added to the storage buffer to stabilize the polymerase.

The RdRps from dsRNA viruses possess at least transcription and replication activities. The former one is required to synthesize (+)ssRNAs to direct production of the viral proteins, while the latter activity is essential for the generation of viral genomic dsRNA on ssRNA template. A transcription activity supporting a semi-conservative mechanism of mRNA synthesis was detected for the recombinant HetRV6 RdRp (Levanova et al., 2021). Both His-tagged and tagless HetRV6 RdRps were able to catalyze RNA replication using native and heterologous ssRNA templates in the absence of oligonucleotide primer and accessory proteins. The enzyme was fully processive on almost

all templates used in the study. In general, recombinant RdRps do not have template-specificity in *in vitro* assays, and catalyze RNA synthesis on any heterologous template that has a suitable 3' end (e.g., contains a specific promoter sequence) or is annealed with a primer. The interaction with other viral proteins are required to gain specificity towards the RNA template (Ferrari et al., 1999; Kao et al., 2001). HetRV6 RdRp was able to initiate RNA replication without any primers, i.e. *de novo*. The *de novo* mechanism of initiation has been demonstrated for all other studied to date RdRps from dsRNA viruses, such as phi6 bacteriophage (Makeyev and Bamford, 2000; Butcher et al., 2001; Laurila et al., 2002) and similar cystoviruses (Yang et al., 2001), picobirnavirus (Collier et al., 2016), reovirus (Tao et al., 2002) and rotavirus (Lu et al., 2008). This mode of initiation is common also for viruses with positive and negative RNA genomes (Kao et al., 2001; van Dijk et al., 2004). In general, d*e novo* initiation requires a higher concentration of one (NTP_i) or two (NTP_i+NTP_{i+1}) first nucleotides, which participate in the formation of a stable initiation complex (Kao et al., 2011; van Dijk et al., 2004; Laurila et al., 2002; Morin et al., 2012). Surprisingly, HetRV6 RdRp operated better in the presence of the increased concentration of the second NTP to be incorporated into the growing chain, ATP (Figure 15). This raises the question of possible internal initiation used by HetRV6 RdRp. Thus, RdRp from a negative-sense RNA virus, vesicular stomatitis virus, can initiate RNA synthesis both at the very 3' end of the template and internally, but the latter mechanism is substantially less efficient (Morin et al., 2012). Further biochemical and structural studies are needed to understand the role of NTP_{i+1} in the formation of the HetRV6 RdRp initiation complex.

I studied the role of divalent cations, Mg^{2+} and Mn^{2+}, on the activity of HetRV6 RdRp. While presence of 2–4 mM Mg^{2+} in the HetRV6 RdRp reaction buffer only slightly enhanced the dsRNA synthesis, Mn^{2+} ions were indispensable for HetRV6 polymerase activity *in vitro* (Figure 13) suggesting its important role for catalysis. Viral RdRps share a catalytic mechanism common for all polynucleotide polymerases, including DNA polymerases, RNA polymerases and reverse transcriptases (Steitz, 1998). Based on the proposed two-metal-ion mechanism (Steitz, 1998; Genna et al., 2018), the addition of an incoming NTP occurs at the 3' end of the nascent strand via S_N2-like phosphoryl transfer reaction. The two catalytic metal ions are coordinated by two invariant aspartate residues in the catalytic center of RdRp. One metal ion (referred to as metal ion A, MeA) decreases the affinity of the primer's 3'-OH group for the hydrogen, assisting in the 3' O^- nucleophilic attack on the α-phosphate of the incoming NTP. The second metal ion (metal ion B, MeB) aids in the leaving of pyrophosphate group, and both metal ions stabilize the pentacovalent transition state (Figure 18). A third divalent cation (metal ion C, MeC) located close to the catalytic site was initially identified in the structure of bacteriophage phi6 RdRp. It was defined as a non-catalytic ion (Butcher et al., 2001), taking part in the correct orientation of the incoming triphosphate in the catalytic site

and increasing flexibility of the enzyme, which is essential for its function (Poranen et al., 2008b). Later the third divalent ion was identified in the structures of other viral RdRps (Mönttinen et al., 2012) and DNA polymerases (e.g., Nakamura et al., 2012; Gao and Yang, 2016). Based on structural, kinetic and mutagenesis studies it seems that MeC plays a key catalytic role and a new "three-metal-ion mechanism" of catalysis for DNA polymerases has been proposed (Gao and Yang, 2016; Tsai, 2019; Yang et al., 2016), which is likely applicable to RNA polymerases. Although there is some argument over the catalytic role of MeC (Tsai, 2019; Wang and Smithline, 2019), nobody denies that MeC ion stabilizes pyrophosphate (Figure 18).

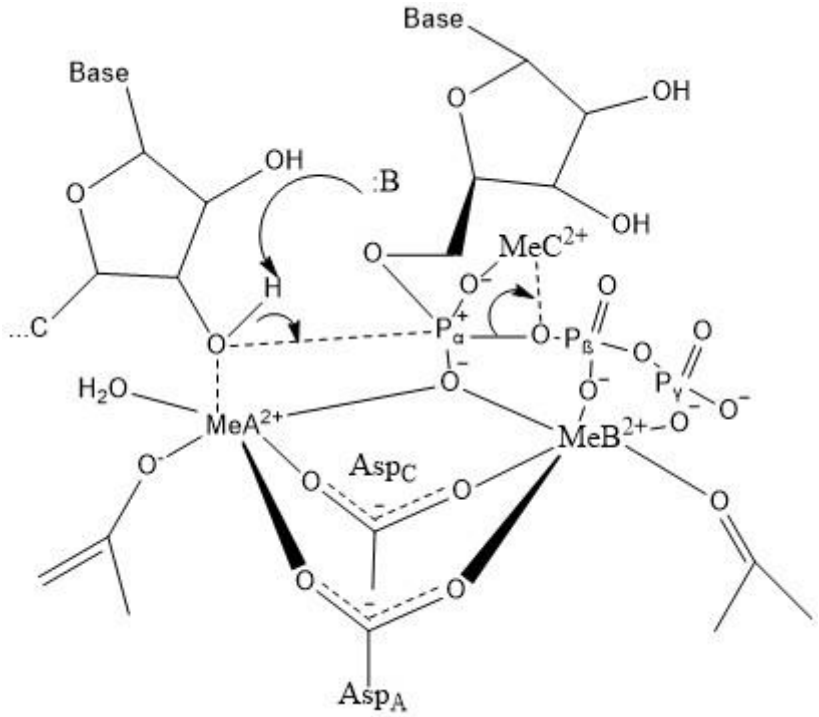

Figure 18. **The presumptive three-metal-ion mechanism of RNA polymerase**. (Reproduced with modifications from (Tsai, 2019) using ChemDraw 19.1).

I optimized the reaction temperature since (Yang et al., 2003) reported that the temperature has a significant effect onto initiation step. Although Heterobasidion host normally grows in the laboratory at room temperature, the polymerization rate at 24°C was rather slow (~11 nt/min) requiring roughly 3 h to replicate a viral genome. This slow rate of replication might be responsible for the cryptic nature of the HetRV6 mycovirus. Although the highest replication rate was observed at 37°C, this temperature is too different from the temperature range at which HetRV6 normally operates. Furthermore, the mycoviruses are typically cleared from their hosts after incubation at 37°C (Vainio et al., 2018). To find a compromise between the natural temperatures of HetRV6 functioning and the RdRp polymerization rate, I conducted polymerization reactions at 30°C.

Similar to several other dsRNA viruses characterized to date (Poranen et al., 2008a; Collier et al., 2016; Graham et al., 2011), HetRV6 RdRp has TNTase activity. The precise function of this activity is still enigmatic. However, it was hypothesized that TNTase activity is required to maintain integrity of the 3' ends of the viral RNA genomes (Ranjith-Kumar et al., 2001).

5. CONCLUSIONS

In the course of the experimental work, which is presented in the thesis and published last year as an article (Levanova et al., 2021), I expressed, purified and characterized *in vitro* activities of HetRV6 RdRp. The purification method that I developed to purify a tagless HetRV6 RdRp permit the preparation of a highly active enzyme free from RNases within three working days. The enzyme is mostly dependent on Mn^{2+} ions rather than Mg^{2+}, active on multiple heterologous templates as a replicase and possesses a TNTase activity. The HetRV6 RdRp was the first biochemically characterized RNA polymerase from the recently established family of dsRNA viruses *Curvulaviridae* and the first polymerase from mycoviruses, in general.

Acknowledgements

Professor Jarkko Hantula and Dr. Eeva Vainio are thanked for the generous gift of the pCR2.1 TOPO HetRV6-RNA1 plasmid. The facilities and expertise of the DNA sequencing service (Viikki, University of Heslinki) and HiLIFE Biocomplex unit at the University of Helsinki, a member of Instruct-ERIC Centre Finland, FINStruct, and Biocenter Finland are gratefully acknowledged.

REFERENCES

1. Aalto, A. P., Sarin, L. P., van Dijk, A. A., Saarma, M., Poranen, M. M., Arumae, U., Bamford, D. H. (2007) Large-scale production of dsRNA and siRNA pools for RNA interference utilizing bacteriophage phi6 RNA-dependent RNA polymerase. *RNA. 13*(3):422-429. doi:10.1261/rna.348307.
2. Ahlquist, P. (2002) RNA-dependent RNA polymerases, viruses, and RNA silencing. *Science. 296*(5571):1270-1273. doi:10.1126/science.1069132.
3. Alphonse, S., Ghose, R. (2017) Cystoviral RNA-directed RNA polymerases: Regulation of RNA synthesis on multiple time and length scales. *Virus Res*. 234:135-152. doi: 10.1016/j.virusres.2017.01.006.
4. Bickle, T. A., Pirrotta, V., Imber, R. (1977) A simple, general procedure for purifying restriction endonucleases. *Nucleic Acids Res*. *4*(8):2561-72. doi: 10.1093/nar/4.8.2561.
5. Bolten, S. N., Rinas, U., Scheper, T. (2018) Heparin: role in protein purification and substitution with animal-component free material. *Appl. Microbiol. Biotechnol. 102*(20):8647–8660. doi:10.1007/s00253-018-9263-3.
6. Bradford, M. M. (1976) A rapid and sensitive method for the quantitation of microgram quantities of protein utilizing the principle of protein-dye binding. *Anal. Biochem*. *72*:248-54. doi: 10.1006/abio.1976.9999.
7. Butcher, S. J., Grimes, J. M., Makeyev, E. V., Bamford, D. H., Stuart, D. I. (2001) A mechanism for initiating RNA-dependent RNA polymerization. *Nature. 410*:235–240. doi: 10.1038/35065653. PMID: 11242087.

8. Černý, J., Černá Bolfíková, B., Valdés, J. J., Grubhoffer, L., Růžek, D. (2014) Evolution of tertiary structure of viral RNA dependent polymerases. *PLoS One*. *9*(5):e96070. doi: 10.1371/journal.pone.0096070.
9. Choi, K. H. (2012) Viral polymerases. *Adv. Exp. Med. Biol. 726*:267-304. doi:10.1007/978-1-4614-0980-9_12.
10. Christiaens, O., Whyard, S., Vélez, A. M., Smagghe, G. (2020) Double-Stranded RNA technology to control insect pests: Current status and challenges. *Front. Plant Sci*. *11*:451. doi: 10.3389/fpls.2020.00451.
11. Collier, A. M., Lyytinen, O. L., Guo, Y. R., Toh, Y., Poranen, M. M., Tao, Y. J. (2016) Initiation of RNA polymerization and polymerase encapsidation by a small dsRNA virus. *PLoS Pathog. 12*(4):e1005523. doi: 10.1371/journal.ppat.1005523.
12. Diaz-Ruiz, J. R., Kaper, J. M. (1978) Isolation of viral double-stranded RNAs using a LiCl fractionation procedure. *Prep. Biochem. 8*(1): 1-17. doi: 10.1080/00327487808068215.
13. Duan, Y., Zeng, M., Jiang, B., Zhang, W., Wang, M., Jia, R., Zhu, D., Liu, M., Zhao, X., Yang, Q., Wu, Y., Zhang, S., Liu, Y., Zhang, L., Yu, Y., Pan, L., Chen, S., Cheng, A. (2019) *Flavivirus* RNA-dependent RNA polymerase interacts with genome UTRs and viral proteins to facilitate *Flavivirus* RNA replication. *Viruses*. *11*(10):929. doi: 10.3390/v11100929.
14. Elbashir, S. M., Harborth, J., Lendeckel, W., Yalcin, A., Weber, K., Tuschl, T. (2001) Duplexes of 21-nucleotide RNAs mediate RNA interference in cultured mammalian cells. *Nature*. *411*(6836):494-8. doi: 10.1038/35078107.
15. Enquist, L. W. (2009) Virology in the 21st century. *J. Virol. 83*(11):5296-5308. doi:10.1128/jvi.00151-09.
16. Ferrari, E., Wright-Minogue, J., Fang, J. W., Baroudy, B. M., Lau, J. Y., Hong, Z. (1999) Characterization of soluble hepatitis C virus RNA-dependent RNA polymerase expressed in *Escherichia coli*. *J. Virol*. *73*(2):1649-54. doi: 10.1128/JVI.73.2.1649-1654.1999.
17. Ferrer-Orta, C., Ferrero, D., Verdaguer, N. (2015) RNA-dependent RNA polymerases of picornaviruses: from the structure to regulatory mechanisms. *Viruses. 8*:4438-60. doi: 10.3390/v7082829.
18. Fletcher, S. J., Reeves, P. T., Hoang, B. T., Mitter, N. (2020) A perspective on RNAi-based biopesticides. *Front. Plant Sci*. *11*:51. doi: 10.3389/fpls.2020.00051.
19. Gao, Y., Yang, W. (2016) Capture of a third Mg^{2+} is essential for catalyzing DNA synthesis. *Science. 352*(6291):1334-7. doi: 10.1126/science.aad9633.
20. Garbelotto, M., Gonthier, P. (2013) Biology, epidemiology, and control of Heterobasidion species worldwide. *Annu. Rev. Phytopathol*. *51*:39-59. doi: 10.1146/annurev-phyto-082712-102225.
21. Genna, V., Donati, E., De Vito, M. (2018) The catalytic mechanism of DNA and RNA polymerases. *ACS Catal*. *8*:11103-11118. doi.org/10.1021/acscatal.8b03363.
22. Gottlieb, P., Strassman, J., Qiao, X., Frilander, M., Frucht, A., Mindich, L. (1992) In vitro packaging and replication of individual genomic segments of bacteriophage phi6 RNA. *J. Virol*. *66*:2611–2616. doi: 10.1128/JVI.66.5.2611-2616.1992.
23. Graham, S. C., Sarin, L. P., Bahar, M. W., Myers, R. A., Stuart, D. I., Bamford, D. H., Grimes, J. M. (2011) The N-terminus of the RNA polymerase from infectious pancreatic necrosis virus is the determinant of genome attachment. *PLoS Pathog. 7*:e1002085. doi: 10.1371/journal.ppat.1002085.
24. Hernández-Soto, A., Chacón-Cerdas, R. (2021) RNAi crop protection advances. *Int. J. Mol. Sci. 22*(22):12148. doi: 10.3390/ijms222212148.
25. Hong, Z., Cameron, C. E., Walker, M. P., Castro, C., Yao, N., Lau, J. Y., Zhong, W. (2001) A novel mechanism to ensure terminal initiation by hepatitis C virus NS5B polymerase. *Virology. 285*(1):6-11. doi:10.1006/viro.2001.0948.
26. Hyder, R., Pennanen, T., Hamberg, L., Vainio, E. J., Piri, T., Hantula, J. (2013) Two viruses of Heterobasidion confer beneficial, cryptic or detrimental effects to their hosts in different situations. *Fungal Ecology. 6*(5):387-396. doi:10.1016/j.funeco.2013.05.005.
27. Jácome, R., Becerra, A., Ponce de León, S., Lazcano, A. (2015) Structural analysis of monomeric RNA-dependent polymerases: Evolutionary and therapeutic implications. *PLoS One. 10*(9):e0139001. doi: 10.1371/journal.pone.0139001.
28. Kao, C. C., Singh, P., Ecker, D. J. (2001) De novo initiation of viral RNA-dependent RNA synthesis. *Virology. 287*(2):251-60. doi: 10.1006/viro.2001.1039.

29. Kolb, V. A.; Makeyev, E. V.; Spirin, A. S. (2000) Co-translational folding of an eukaryotic multidomain protein in a prokaryotic translation system. *J. Biol. Chem*. *275*:16597–16601. doi: 10.1074/jbc.M002030200.
30. Laemmli, U. K. (1970) Cleavage of structural proteins during the assembly of the head of bacteriophage T4. *Nature*. *227*(5259):680-5. doi: 10.1038/227680a0.
31. Laurila, M. R. L., Makeyev, E. V., Bamford, D. H. (2002) Bacteriophage phi6 RNA-dependent RNA polymerase: molecular details of initiating nucleic acid synthesis without primer. *J. Biol. Chem*. *277*: 17117–17124. doi:10.1074/jbc.M111220200
32. Levanova, A. A., Lampi, M., Kalke, K., Hukkanen, V., Poranen, M. M., Eskelin, K. (2022) Native RNA purification method for small RNA molecules based on asymmetrical flow field-flow fractionation. *Pharmaceuticals* (Basel). *15*(2):261. doi: 10.3390/ph15020261.
33. Levanova, A. A., Vainio, E. J., Hantula, J., Poranen, M. M. (2021) RNA-dependent RNA polymerase from Heterobasidion RNA virus 6 is an active replicase in vitro. *Viruses. 13*(9):1738. doi: 10.3390/v13091738.
34. Liew, O. W., Ching Chong, J. P., Yandle, T. G., Brennan, S. O. (2005) Preparation of recombinant thioredoxin fused N-terminal proCNP: Analysis of enterokinase cleavage products reveals new enterokinase cleavage sites. *Protein Expr. Purif. 41*(2):332-40. doi: 10.1016/j.pep.2005.03.006.
35. Lu, X., McDonald, S. M., Tortorici, M. A., Tao, Y. J., Vasquez-Del Carpio, R., Nibert, M. L., Patton, J. T., Harrison, S. C. (2008) Mechanism for coordinated RNA packaging and genome replication by rotavirus polymerase VP1. *Structure. 16*(11): 1678–1688. doi: 10.1016/j.str.2008.09.006.
36. Makeyev, E. V., Bamford, D. H. (2000) Replicase activity of purified recombinant protein P2 of double-stranded RNA bacteriophage phi6. *EMBO J. 19*(1):124-33. doi: 10.1093/emboj/19.1.124.
37. Márquez, L. M., Redman, R. S., Rodriguez, R. J., Roossinck, M. J. (2007) A virus in a fungus in a plant: three-way symbiosis required for thermal tolerance. *Science*. *315*(5811):513-5. doi: 10.1126/science.1136237.
38. Mietzsch, M., Agbandje-McKenna, M. (2017) The Good That Viruses Do. *Ann. Rev. Virol. 4*(1): iii-v. doi: 10.1146/annurev-vi-04-071217-100011.
39. Mönttinen, H. A. M., Ravantti, J. J., Poranen, M. M. (2021) Structure unveils relationships between RNA virus polymerases. *Viruses*. *13*(2):313. doi: 10.3390/v13020313.
40. Mönttinen, H. A., Ravantti, J. J., Poranen, M. M. (2012) Evidence for a non-catalytic ion-binding site in multiple RNA-dependent RNA polymerases. *PLoS One*. *7*(7):e40581. doi: 10.1371/journal.pone.0040581.
41. Morin, B., Kranzusch, P. J., Rahmeh, A. A., Whelan, S. P. (2013) The polymerase of negative-stranded RNA viruses. *Curr. Opin. Virol*. *3*(2):103-10. doi: 10.1016/j.coviro.2013.03.008.
42. Morin, B., Rahmeh, A. A., Whelan, S. P. (2012) Mechanism of RNA synthesis initiation by the vesicular stomatitis virus polymerase. *EMBO J*. *31*(5):1320-9. doi: 10.1038/emboj.2011.483.
43. Nakamura, T., Zhao, Y., Yamagata, Y., Hua, Y. J., Yang, W. (2012) Watching DNA polymerase η make a phosphodiester bond. *Nature*. *487*(7406):196-201. doi: 10.1038/nature11181.
44. Novoa, R. R., Calderita, G., Arranz, R., Fontana, J., Granzow, H., Risco, C. (2005) Virus factories: associations of cell organelles for viral replication and morphogenesis. *Biol. Cell. 97*(2), 147-172. doi:10.1042/bc20040058.
45. Nwokeoji, A. O., Kung, A. W., Kilby, P. M., Portwood, D. E., Dickman, M. J. (2017) Purification and characterisation of dsRNA using ion pair reverse phase chromatography and mass spectrometry. *J. Chromatogr. A. 1484*:14-25. doi: 10.1016/j.chroma.2016.12.062.
46. Paul, A.V., Wimmer, E. (2015) Initiation of protein-primed picornavirus RNA synthesis. *Virus Res*. *206*:12-26. doi: 10.1016/j.virusres.2014.12.028.
47. Poranen, M. M., Koivunen, M. R., Bamford, D. H. (2008a) Nontemplated terminal nucleotidyltransferase activity of double-stranded RNA bacteriophage phi6 RNA-dependent RNA polymerase. *J. Virol*. *82*:9254–9264.
48. Poranen, M. M., Paatero, A. O., Tuma, R., Bamford, D. H. (2001) Self-assembly of a viral molecular machine from purified protein and RNA constituents. *Mol. Cell. 7*(4), 845-854. doi: 10.1016/s1097-2765(01)00228-3.
49. Poranen, M. M., Salgado, P. S., Koivunen, M. R., Wright, S., Bamford, D. H., Stuart, D. I., Grimes, J. M. (2008b) Structural explanation for the role of Mn^{2+} in the activity of phi6 RNA-dependent RNA polymerase. *Nucleic Acids Res.* 36(20):6633-44. doi: 10.1093/nar/gkn632.

50. Ranjith-Kumar, C. T., Gajewski, J., Gutshall, L., Maley, D., Sarisky, R. T., Kao, C. C. (2001) Terminal nucleotidyl transferase activity of recombinant Flaviviridae RNA-dependent RNA polymerases: Implication for viral RNA synthesis. *J. Virol*. *75*:8615–8623.
51. Riguero, V., Clifford, R., Dawley, M., Dickson, M., Gastfriend, B., Thompson, C., Wang, S. C., O'Connor, E. (2020) Immobilized metal affinity chromatography optimization for poly-histidine tagged proteins. *J. Chromatogr. A. 11*:1629:461505. doi: 10.1016/j.chroma.2020.461505.
52. Romanovskaya, A., Sarin, L. P., Bamford, D. H., Poranen, M. M. (2013) High-throughput purification of double-stranded RNA molecules using convective interaction media monolithic anion exchange columns. *J. Chromatogr. A. 1278:*54-60. doi:10.1016/j.chroma.2012.12.050.
53. Saw, P. E., Song, E. W. (2020) siRNA therapeutics: a clinical reality. *Sci. China Life Sci. 63*(4):485-500. doi: 10.1007/s11427-018-9438-y.
54. Shahravan, S. H., Qu, X., Chan, I. S., Shin, J. A. (2008) Enhancing the specificity of the enterokinase cleavage reaction to promote efficient cleavage of a fusion tag. *Protein Expr. Purif*. *59*(2):314-319. doi:10.1016/j.pep.2008.02.015.
55. Shwed, P. S., Dobos, P., Cameron, L. A., Vakharia, V. N., Duncan, R. (2002) Birnavirus VP1 proteins form a distinct subgroup of RNA-dependent RNA polymerases lacking a GDD motif. *Virology*. *296*(2):241-50. doi: 10.1006/viro.2001.1334.
56. Singh, L., Jones, K. W. (1984) The use of heparin as a simple cost-effective means of controlling background in nucleic acid hybridization procedures. *Nucleic Acids Res*. *12*(14):5627-38. doi: 10.1093/nar/12.14.5627.
57. Staby, A., Sand, M. B., Hansen, R. G., Jacobsen, J. H., Andersen, L. A., Gerstenberg, M., Bruus, U. K., Jensen, I. H. (2005) Comparison of chromatographic ion-exchange resins IV. Strong and weak cation-exchange resins and heparin resins. *J. Chromatogr. A*. *1069*(1):65-77. doi: 10.1016/j.chroma.2004.11.094.
58. Steitz, T. A. (1998) A mechanism for all polymerases. *Nature*. *391*(6664):231-2. doi: 10.1038/34542. PMID: 9440683.
59. Stellwagen, E. (2001) Dye affinity chromatography. *Curr. Protoc. Protein Sci*. Chapter 9.2. doi: 10.1002/0471140864.ps0902s00.
60. Sternbach, H., Engelhardt, R., Lezius, A. G. (1975) Rapid isolation of highly active RNA polymerase from *Escherichia coli* and its subunits by matrix-bound heparin. *Eur. J. Biochem*. *60*(1):51-5. doi: 10.1111/j.1432-1033.1975.tb20974.x.
61. Takeshita, D., Tomita, K. (2012) Molecular basis for RNA polymerization by Qβ replicase. *Nat. Struct. Mol. Biol*. *19*(2):229-37. doi: 10.1038/nsmb.2204.
62. Tao, Y., Farsetta, D. L., Nibert, M. L., Harrison, S. C. (2002) RNA synthesis in a cage–structural studies of reovirus polymerase λ3. *Cell*. *111*:733–745. doi: 10.1016/s0092-8674(02)01110-8.
63. Tsai, M. D. (2019) Catalytic mechanism of DNA polymerases-two metal ions or three? *Protein Sci*.*28* (2):288-291. doi: 10.1002/pro.3542.
64. Vainio, E. J., Chiba, S., Nibert, M. L., Roossinck, M. J., Sabanadzovic, S., Suzuki, N., Xie, J. (2020) Taxonomy Proposal 2020: Create one new family *Curvulaviridae*, one new genus *Orthocurvulavirus* and eight new species. Available online: https://talk.ictvonline.org/files/ictv_official_taxonomy_updates_since_the_8th_report/m/fungal-official/11111 (accessed on 19 March 2022).
65. Vainio, E. J., Hakanpaa, J., Dai, Y. C., Hansen, E., Korhonen, K., Hantula, J. (2011) Species of Heterobasidion host a diverse pool of partitiviruses with global distribution and interspecies transmission. *Fungal Biol. 115*(12):1234-1243. doi:10.1016/j.funbio.2011.08.008.
66. Vainio, E. J., Hyder, R., Aday, G., Hansen, E., Piri, T., Dogmus-Lehtijarvi, T., Lehtijärvi, A., Korhonen, K., Hantula, J. (2012) Population structure of a novel putative mycovirus infecting the conifer root-rot fungus *Heterobasidion annosum* sensu lato. *Virology. 422*(2):366-376. doi:10.1016/j.virol.2011.10.032.
67. Vainio, E. J., Jurvansuu, J., Hyder, R., Kashif, M., Piri, T., Tuomivirta, T., Poimala, A., Xu, P., Mäkelä, S., Nitisa, D., Hantula, J. (2018) Heterobasidion partitivirus 13 mediates severe growth debilitation and major alterations in the gene expression of a fungal forest pathogen. *J. Virol. 92*: e01744–17. doi: 10.1128/JVI.01744-17.
68. van Dijk, A. A., Makeyev, E. V., Bamford, D. H. (2004) Initiation of viral RNA-dependent RNA polymerization. *J. Gen. Virol*. *85*(Pt 5):1077-1093. doi: 10.1099/vir.0.19731-0.

69. Venkataraman, S., Prasad, B. V. L. S., Selvarajan, R. (2018) RNA-dependent RNA polymerases: insights from structure, function and evolution. *Viruses. 10*(2):76. doi: 10.3390/v10020076.
70. Voyles, B. A. (2002) The biology of viruses (2nd ed.): McGraw-Hill Science/Engineering/Math.
71. Wang, J., Smithline, Z. B. (2019) Crystallographic evidence for two-metal-ion catalysis in human pol η. *Protein Sci. 28*(2):439-447. doi: 10.1002/pro.3541.
72. Xiong, S., Zhang, L., He, Q. Y. (2008) Fractionation of proteins by heparin chromatography. *Methods Mol. Biol. 424*:213-21. doi: 10.1007/978-1-60327-064-9_18.
73. Yang, H., Gottlieb, P., Wei, H., Bamford, D. H., Makeyev, E. V. (2003) Temperature requirements for initiation of RNA-dependent RNA polymerization. *Virology*. *314*(2):706-15. doi: 10.1016/s0042-6822(03)00460-4.
74. Yang, H., Makeyev, E. V., Bamford, D. H. (2001) Comparison of polymerase subunits from double-stranded RNA bacteriophages. *J. Virol*. *75*(22):11088-95. doi: 10.1128/JVI.75.22.11088-11095.2001.
75. Yang, W., Weng, P. J., Gao, Y. (2016) A new paradigm of DNA synthesis: three-metal-ion catalysis. *Cell Biosci*. *6*(1):51. doi: 10.1186/s13578-016-0118-2.

APPENDICES

Appendix 1.Oligonucleotodes used in the study (modified from Levanova et al., 2021)

Name	Sequence[1,2]	Description	Reference
Fwd _HRV6_NcoI	GCA**CCATGG**CTTCAACTCCATCCTCATTTCAG	Cloning primer, NcoI site	Levanova et al., 2021
Rev_ HRV6_HindIII	GCA**AAGCTT**CTATCCTCGCCGCTCGGATCAAT	Cloning primer, HindIII site	Levanova et al., 2021
HRV6_T7_Fwd_full	TAATACGACTCACTATAGGGCAATAAAGAAGGGACTCAGG	Preparation of cDNA template for HetRV6 RNA1$^+$ production	Levanova et al., 2021
HRV6_Rev_full	CAGCAACCCGAGGACCTTC	Preparation of cDNA template for HetRV6 RNA1$^+$ production	Levanova et al., 2021
3' end	AGAGAGAGAGCCCCCGA	Primer for preparation of cDNA templates for phi6 s$^+$, Δs$^+$ RNA, and all luc ssRNAs production	Yang et al., 2001
T7-1	CGCGTAATACGACTCACTATAG	Preparation of cDNA template for phi6 s$^+$ and Δs$^+$ RNA production	Yang et al., 2001
3′end_6	GGGAGAGAGAGAGCCCCCGA	Preparation of cDNA template for phi6 Δs$^+_{CCC}$ RNA production	Wright et al., 2012
PBV2_T7_Fwd	CGCGTAATACGACTCACTATAG TAAAATTTTCGAATTTTATAATAATTAAG	Preparation of cDNA template for PBV RNA2$^+$ production	Collier et al., 2016
PBV2_Rev	GCAGTTGGGACTGTTAGTCCCAATG	Preparation of cDNA template for PBV RNA2$^+$ production	Collier et al., 2016
pT7_3'end	TAAGCTTGGGCTGCAGGT	Preparation of cDNA template for luc$^+$_0 RNA	Yang et al., 2001
pT7_3'end_2	CTAAGCTTGGGCTGCAGGT	Preparation of cDNA template for luc$^+$_2RNA	Yang et al., 2001
pT7_3'end_3	GTAAGCTTGGGCTGCAGGT	Preparation of cDNA template for luc$^+$_3 RNA	Yang et al., 2001
pT7_3'end_4	TTAAGCTTGGGCTGCAGGT	Preparation of cDNA template for luc$^+$_4 RNA	Yang et al., 2001

[1] Restriction enzyme cut sites are in bold

[2] T7 polymerase promoter sequence is underlined

Appendix 2. SsRNA templates used in the polymerase assays (modified from Levanova et al., 2021)

SsRNA name	Plasmid used for preparation	3'-end sequence; description	Length, nt
HetRV6 RNA1^{+}	pCR2.1-TOPO-HetRV6-RNA1 (Vainio et al., 2012)	5'-…GCUG-3'; native HetRV6 RNA1^{+}	2050
PBV2^{+}	pMA-RQ_PBV2 (Collier et al., 2016)	5'-…UAC-3'; native human PBV RNA2^{+}	1745
phi6 s^{+}	pLM659 (Gottlieb et al., 1992)	5'-…CUCU-3'; native phi6 S-segment ssRNA	2948
phi6 Δs^{+} (phi6 S-segment Δ593—2830)	pEM15 (Makeyev and Bamford, 2000)	5'-…CUCU-3'; s^{+} with deletion of nts 593—2830	710
phi6 Δs$^{+}_{13}$	the same	5'-…AUCCCC-3'; sΔ^{+} with a 13-nt-long extension forming a hairpin at the 3'-end	723
phi6 Δs$^{+}_{CCC}$	the same	5'-…CUCUCUCCC-3'; Δs^{+} with three nt extension at the 3'-end	713
phi6 Δs$^{+}_{HP}$	pEM19 (Laurila et al., 2002)	5'-…UUCGCCCC-3'; sΔ^{+} with a 13-nt stable tetraloop at the 3'-end	725
luc^{+}_0	pT7luc (Kolb et al., 2000)	5'…UUA-3'; firefly luciferase mRNA	1824
luc^{+}_2	the same	5'…UUAG-3'; firefly luciferase with 3'G extension	1825
luc^{+}_3	the same	5'…UUAC-3'; firefly luciferase with 3'C extension	1825
luc^{+}_4	the same	5'…UUAA-3'; firefly luciferase with 3'A extension	1825

Appendix 3. A fragment of pET-32b(+) expression region at the N-terminus of the HetRV6 RdRp[1]

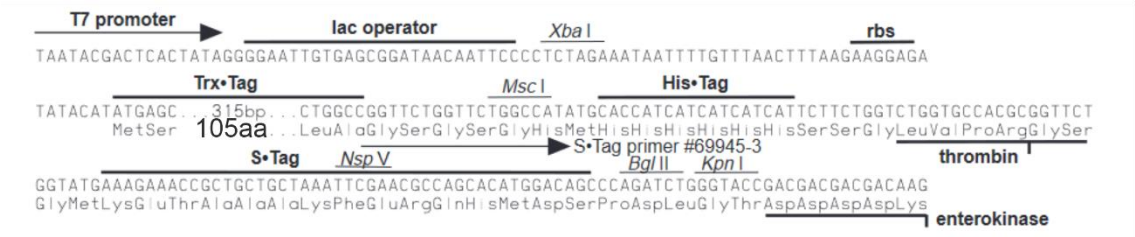

[1]- the full map of the pET-32a-c(+) vectors is accessible via https://www.helmholtz-muenchen.de/fileadmin/PEPF/pET_vectors/pET-32a-c_map.pdf